Published in final edited form as:
J Immunol. 2013 August 15; 191(4): . doi:10.4049/jimmunol.1300922.

Induction of AID-targeting adaptor 14-3-3γ is mediated by NF-κB-dependent recruitment of CFP1 to the 5′-CpG-3′-rich *14-3-3*γ promoter and is sustained by E2A

Thach Mai, **Egest J. Pone**, **Guideng Li**, **Tonika S. Lam**, **J'aime Moehlman**, **Zhenming Xu**, and **Paolo Casali**
Institute for Immunology, School of Medicine, University of California, Irvine, CA 92697-4120.

Abstract

Class switch DNA recombination (CSR) crucially diversifies antibody biological effectors functions. 14-3-3γ specifically binds to the 5′-AGCT-3′ repeats in the *IgH* locus switch (S) regions. By directly interacting with the C-terminal region of activation-induced cytidine deaminase (AID), 14-3-3γ targets this enzyme to S regions to mediate CSR. Here, we showed that 14-3-3γ was expressed in germinal center B cells *in vivo* and induced in B cells by T-dependent and T-independent primary CSR-inducing stimuli *in vitro* in humans and mice. Induction of 14-3-3γ was rapid, peaking within 3 h of stimulation by lipopolysaccharides (LPS), and sustained over the course of AID and CSR induction. It was dependent on recruitment of NF-κB to the *14-3-3*γ gene promoter. The NF-κB recruitment enhanced the occupancy of the CpG island within the *14-3-3*γ promoter by CFP1, a component of the COMPASS histone methyltransferase complex, and promoter-specific enrichment of histone 3 lysine 4 trimethylation (H3K4me3), which is indicative of open chromatin state and marks transcription-competent promoters. NF-κB also potentiated the binding of B cell lineage-specific factor E2A to an E-box motif located immediately downstream of the two closely-spaced transcription start sites (TSSs) for sustained 14-3-3γ expression and CSR induction. Thus, 14-3-3γ induction in CSR is enabled by the CFP1-mediated H3K4me3 enrichment in the promoter, dependent on NF-κB and sustained by E2A.

Introduction

B lymphocytes are activated by a variety of microorganisms, such as bacteria and viruses, to proliferate and differentiate into plasma cells and memory B cells (1–3). T-dependent antibody responses depend on engagement of B cell CD40 by trimeric CD154 expressed on the surface of T helper (T_H) cells (4, 5). T-independent antibody responses are elicited by antigens that trigger weak or no T cell responses and are boosted by (innate immune) Toll-like receptors (TLRs), which are engaged by microbe-associated molecular patterns (MAMPs) (6–8). TLR-signaling also plays an important role in T-dependent responses before the emergence of specific T_H cells, and can synergize with B cell receptor (BCR)-signaling to induce B cell proliferation and differentiation (9).

The maturation of the antibody response depends on immunoglobulin (Ig) somatic hypermutation (SHM) and class switch DNA recombination (CSR). SHM inserts mainly point-mutations in DNA of the V(D)J regions, thereby providing the structural substrate for the positive selection by antigen of higher affinity antibody mutants (10, 11). CSR replaces

Address correspondence to Dr. Paolo Casali (pcasali@uci.edu) or Dr. Zhenming Xu (zhenming@uci.edu).

Disclosures
The authors declare no competing financial interests.

an IgH constant (C_H) region, e.g., Cμ, with a downstream C_H region (Cγ, Cα or Cε), thereby diversifying the biological effector functions of an antibody without changing its specificity or affinity for antigen (12). Both SHM and CSR require activation-induced cytidine deaminase (AID), which is specifically expressed in activated B cells. AID deaminates deoxycytosines in V(D)J regions and switch (S) region DNA for SHM and CSR, respectively (13–15). High densities of deoxyuracils, as generated following AID-mediated DNA deamination (16), are processed by uracil DNA glycosylase (Ung), as recruited by Rev1 for the generation of double-stranded DNA breaks (DSBs) in the upstream (donor) and downstream (acceptor) S regions (17, 18). Resolution of these DSBs results in looping out of the intervening DNA as an S circle, formation of S-S junction, leading to juxtaposition of the expressed V_HDJ_H DNA to the downstream C_H DNA (19, 20).

Induction of CSR requires “primary” and “secondary” stimuli (12). Primary stimuli comprise T-dependent and T-independent stimuli: (i) engagement of CD40 constitutively expressed on B cells by CD154 expressed on activated T cells; (ii) dual engagement of TLRs and BCR, as effected by MAMPs and repetitive microbial antigenic epitopes, respectively (9, 21); and (iii) dual engagement of TLRs and TACI (TACI is engaged by BAFF or APRIL secreted from activated immune cells or epithelial cells) or BCR and TACI (7, 9, 22). The only known microbial component that can directly induce efficient CSR is bacterial lipopolysaccharides (LPS), owing to the ability of LPS to engage TLR4 (on mouse B cells) through the lipid A moiety and to crosslink the BCR of a large proportion of B cells through the repetitive polysaccharidic moiety, O-antigen (8). Primary stimuli induce expression of AID and other important CSR-factors through activation of NF-κB, HoxC4 and other transcription factors (14, 23). They also enable secondary stimuli, i.e., cytokines that include IL-4 and TGF-β (and IFN-γ in the mouse) to induce germline I_H-S-C_H transcription and histone modifications in the donor and acceptor S regions (24–28), thereby directing CSR to predetermined Ig isotypes. IL-4 and TGF-β can enhance induction of AID by primary stimuli (14).

14-3-3 adaptor proteins (seven isoforms: 14-3-3β, 14-3-3ε, 14-3-3γ, 14-3-3η, 14-3-3σ, 14-3-3τ and 14-3-3ζ) specifically bind the evolutionarily conserved 5′-AGCT-3′ repeats in S region DNA and target the S regions that will undergo recombination through interaction with the combinatorial histone modifications H3K9acS10ph (29, 30). 14-3-3 adaptors recruit and/or stabilize AID to transcribed S regions through direct protein-protein interaction (29). 14-3-3 interaction with AID depends on the AID C-terminal region, which is dispensable for the AID DNA deamination activity but critical for AID to mediate CSR (31, 32). As we have previously shown, CSR is significantly reduced in *14-3-3γ*$^{-/-}$ B cells, indicating this isoform plays a critical role in the AID targeting in CSR (29).

As suggested by our previous findings, 14-3-3 proteins, like AID, are expressed in a B cell differentiation stage-specific fashion, such as in germinal center B cells, in which CSR occurs at a high level, and in B cells induced to undergo CSR by CD154 or LPS plus IL-4 (29). While significant advances have been made in the understanding of the regulation of the AID gene (*AICDA*/*Aicda*) expression, including the role of HoxC4 and NF-κB transcription factors and role of microRNAs (33), how the expression of 14-3-3γ, as a critical AID-targeting CSR factor, is regulated remains unclear. Here, we have analyzed induction of 14-3-3γ by the same stimuli that induce AID and CSR and induction kinetics. Using comparative gene analysis and 5′-RACE, we have mapped the *14-3-3γ* transcription start sites (TSSs) and identified unique and evolutionarily conserved features of the *14-3-3γ* promoter. Using chromatin immunoprecipitation (ChIP), we have also addressed the molecular mechanisms underlying 14-3-3γ induction by analyzing *14-3-3γ* locus-wide recruitment of transcription factors NF-κB and E2A and epigenetic changes. Finally, we have used multiple molecular approaches, including small molecule antagonistic

compounds, knockout (KO) mice, inhibitory proteins and a luciferase reporter system involving the *14-3-3γ* promoter, to define the modality of NF-κB and E2A-mediated 14-3-3γ induction.

Materials and Methods

Human B cells

Single cell suspensions of $IgD^{-}CD38^{+}CD19^{+}$ germinal center B cells and $IgD^{+}CD38^{-}CD19^{+}$ naive B cells were prepared from human tonsil surgical specimens, stained with fluorophore-conjugated mAbs to CD19, IgD and CD38 (BD Biosciences) and sorted using a MoFlo® (Beckman Coulter). Human peripheral blood mononuclear cells (PBMCs) were prepared from buffy coat (obtained from the Blood Bank of UC Irvine Medical Center) by a Ficoll-Paque Plus® density gradient (GE Healthcare). Naïve IgD^{+} B cells were then purified using a MACS®-based naïve B cell isolation kit (Miltenyi) following the manufacturer's instructions (typically yielding over 98% of IgD^{+} B cells and no IgG^{+} or IgA^{+} B cells) and cultured at 5×10^{5} cell/ml in RPMI-1640 (Invitrogen) supplemented with FBS (10% v/v, Hyclone), penicillin-streptomycin (1% v/v, Invitrogen), amphotericin B (1% v/v, Invitrogen) and 50 μM β-mercaptoethanol (FBS-RPMI). IgD^{+} B cells were stimulated with an agonistic mAb to human CD40 (1 U/ml, clone G28-5, ATCC) plus recombinant human IL-4 (30 ng/ml, Genzyme). All protocols were in accordance to the rules and regulations of the UC Irvine Institutional Regulatory Board (IRB).

Mouse B cells

Spleen and lymph node B cells were prepared as described (8). B cells were cultured (5×10^{5} cell/ml in FBS-RPMI) in the presence of: CD154 (3 U/ml, mouse CD154-containing membrane fragments of baculovirus-infected Sf21 insect cells (23, 29)), LPS (5 μg/ml, from *E. coli*, serotype 055:B5 and deproteinized by chloroform extraction, Sigma-Aldrich), TLR7 ligand R-848 (30 ng/ml, Invivogen) or TLR9 ligand CpG ODN1826 with a phosphorothioate backbone (CpG ODN, 1 μM, sequence 5′-TCCATGACGTTC CTGACGTT-3′; Operon). IL-4 (3 ng/ml, R&D Systems) or anti–δ mAb (clone 11–26)–conjugated dextran (anti–δ mAb/dex, 10 ng/ml; Fina Biosolutions) were added as indicated. For inhibition of IKK-2 using [5-(p-fluorophenyl)-2-ureido] thiophene-3-carboxamide (TPCA-1, EMD Millipore), B cells were pre-treated with 1 μM TPCA-1 for 1 h in FBS-RPMI before stimuli were added.

Retroviral transduction

The S-003 and S003-Id3 retroviral vectors were kindly provided by Dr. C. Murre (34) (University of California, San Diego). For the generation of retrovirus, retroviral constructs were transfected along with the pCL–Eco retrovirus–packaging vector (Imgenex) into HEK293T cells using the ProFection Mammalian Transfection System® (Promega). Transfected cells were cultured in FBS-RPMI in the presence of chloroquine (25 μM) for 8 h. After the removal of chloroquine, retrovirus-containing culture supernatants were harvested every 12 h. For transduction and CSR analysis, mouse B cells were activated with LPS for 24 h and then centrifuged at 500 *g* together with viral particles in the presence of 6 μg/ml polybrene (Sigma-Aldrich) for 90 min at 25°C. Transduced B cells were then cultured in virus-free FBS-RPMI in the presence of LPS plus IL-4 for 48 h for transcript analysis, or for 72 h for flow cytometry analysis of surface IgG1 and B220 expression in GFP^{+} B cells (GFP translation is initiated by the IRES in the S-003 vector; GFP^{+} B cells indicating transduced B cells), as we described (23, 29). Dead ($7\text{–}AAD^{+}$) cells were excluded from analysis.

5′-Rapid amplification of cDNA ends (5′-RACE)

FirstChoice® RLM-RACE kit (Ambion) was used according to manufacturer's specification to identify the TSS(s) of the *14-3-3γ* gene. Briefly, total RNA was extracted from mouse B cells cultured with LPS plus IL-4 for 24 h and then treated with calf alkaline intestinal phosphatase (CIP) at 37°C for 1 h to remove the 5′-phosphate group from RNA and DNA molecules degraded at their 5′ ends. After quenching by 4 M of amonium acetate and purification by phenol/choloroform extraction, RNA was treated at 37°C for 1 h with tobacco acid pyrophosphatase (TAP), which cleaves the 7′-methylguanosine cap (m7′G cap) of mRNA, to expose the 5′-phosphate group in mRNA molecules originally with an intact m7′G cap (mRNA molecules originally degraded at 5′ end thus would not have 5'-phosphate group). After a 5′-RACE RNA adaptor was linked to the newly exposed 5′-phosphate group, mRNA molecules were reverse transcribed for amplification of the 5′ end of *14-3-3γ* cDNA by two rounds of PCR involving 5′-RACE adaptor-specific outer and nested inner primers (both forward primers) and *14-3-3γ*–specific outer primer (reverse primer, priming DNA about 230-nt DNA downstream of the putative promoter) and inner primer (nested reverse primer, priming DNA about 90-nt DNA downstream of the putative promoter) (primers are listed in Supplemental Table SI). Amplified *14-3-3γ*–specific cDNA was analyzed by agarose gel electrophoresis and cloned into the pCR®-Blunt II-TOPO® vector (Invitrogen) for sequencing of individual cDNA molecules.

Transcript analysis by real-time qRT-PCR

RNA was extracted from B cells (5×10^6) using RNeasy Mini Kit (Qiagen) according to the manufacturer's instruction. First-strand cDNA was synthesized from 2 μg of RNA using the SuperScript™ III System with an oligo-dT primer (Invitrogen) and then analyzed by real-time qPCR using appropriate primers (Supplemental Table S1) and SYBR Green (Dynamo HS kit; New England Biolabs). PCR was performed in the MyiQ Single-color Real-Time PCR Detection System (Bio-Rad Laboratories) according to the following protocol: 95°C for 30 s, 40 cycles of 95°C for 10 s, 60°C for 30 s, 72°C for 30 s. Melting curve analysis was performed at 72°–95°C. The ΔΔCt method was used to analyze levels of transcripts and data were normalized to the level of *Cd79b*, which encodes the BCR Igβ chain constitutively expressed in B cells.

Chromatin immunoprecipitation (ChIP) assays

ChIP assays were performed as we described (35). Briefly, B cells (1×10^7) were treated with 1% formaldehyde in PBS at 25°C for 10 min to crosslink chromatin. After quenching with 100 mM of glycine (pH 8.0) and washing with cold PBS containing a cocktail of protease inhibitors (Sigma-Aldrich), B cells were resuspended in SDS-lysis buffer (20 mM Tris-HCl, pH 8.0, 200 mM NaCl, 2 mM EDTA, 0.1% (w/v) sodium deoxycholate, 0.1% (w/v) SDS, and protease inhibitor cocktail). Chromatin was sonicated to yield approximately 200–600-bp DNA fragments, pre-cleared with agarose beads conjugated with protein A (Pierce) and then incubated with a polyclonal rabbit Ab to CFP1, H3K4me1, H3K4me3, p65, p52 or E2A at 4°C (antibodies are listed in Supplemental Table SII). After overnight incubation, immune complexes were isolated using agarose-beads conjugated with protein A, washed and eluted in buffer containing 50 mM Tris-HCl, 0.5% SDS, 200 mM NaCl and 100 μg/ml Proteinase K (pH 8.0). Eluates were incubated at 65°C for 4 h to reverse formaldehyde crosslinks. DNA was purified using a QIAquick PCR purification column (Qiagen) and analyzed by real-time qPCR using specific primers. For ChIP assays involving anti–NF-κB (p65 or p52) Ab, B cells were subjected to crosslinking with disuccinimidyl glutarate (1 mM, Pierce) for 30 min and then washing with cold PBS immediately before crosslinking with formaldehyde.

For two-step ChIP assays, crosslinked protein–DNA complexes were immunoprecipitated by the first Ab, as captured by protein A agarose beads. After washing and centrifugation, the pelleted beads were resuspended in 40 μl freshly made Re-ChIP buffer (16.7 mM Tris-HCl, pH 8.0, 167 mM NaCl, 1.2 mM EDTA, 1.1% (v/v) Triton X-100, 10 mM DTT and protease inhibitor cocktail) and incubated at 37 °C for 30 m. The supernatant (40 μl) was diluted with 1.6 ml buffer (16.7 mM Tris-HCl, pH 8.0, 167 mM NaCl, 1.2 mM EDTA, 1.1% (V/V) Triton X-100) supplemented with 100 μg purified salmon sperm DNA, 100 μg purified yeast tRNA (Invitrogen) and 1 mg purified BSA (New England Biolabs) and precipitated by the second antibody. The procedures following the second immunoprecipitation, including binding to agarose beads bearing protein A, reverse crosslinking and DNA purification, were the same as for regular ChIP assays.

Luciferase reporter assays

A 310–bp DNA sequence encompassing the two *14-3-3*γ TSSs (−270-bp – +40-bp) was amplified by PCR from mouse genomic DNA using specific primers and cloned into the pGL3-basic firefly (*Phttinus pyrelis*) luciferase gene reporter vector (Promega). Mutant gene reporter constructs containing a truncated *14-3-3*γ promoter were generated by PCR-based mutagenesis and confirmed by DNA sequencing. Reporter constructs were co-transfected with the pRL-TK vector (Promega), which drives constitutive expression of *Renilla reniformis* luciferase, into mouse CH12F3 B cells by electroporation (250V and 900 Ω) in a Gene Pulser II™ (BioRad), yielding typically more than 40% transfection efficiency. Transfected CH12F3 B cells were then cultured in FBS-RPMI in the presence of CD154, IL-4 and TGF-β for 3 h or 24 h. Promoter activation was quantified by normalizing the firefly luciferase activity to the *Renilla* luciferase activity using the Dual-Luciferase Reporter Assay System® (Promega) according to manufacturer's instructions.

Immunoblotting

B cells (1×10^6) were harvested by centrifugation at 500 *g* for 5 m, resuspended in 0.5 ml of lysis buffer (20 mM Tris-Cl, pH 7.5, 150 mM NaCl, 0.5 mM EDTA, 1% (v/v) NP-40) supplemented with phosphatase inhibitors sodium pyrophosphate (1 mM), NaF (10 mM), $NaVO_3$ (1 mM) and a cocktail of protease inhibitors (Sigma-Aldrich). Cell lysates were separated by SDS–PAGE and transferred onto nitrocellulose membranes for immunoblotting involving specific Abs. Membranes were then stripped with 200 mM glycine (pH 2.5), equilibrated in PBS, and subjected to immunoblotting with an anti–β–actin mAb (antibodies are listed in Supplemental Table SII).

Intracellular staining analysis of 14-3-3γ expression in B cells

B cells (1×10^6) were fixed and permeabilized using the Cytofix/Cytoperm™ Fixation and Permeabilization solution (BD Biosciences) following the manufacturer's instructions. After washing with PBS, cells were resuspended in 50 μl of the antibody diluent solution containing a polyclonal Ab specific for 14-3-3γ (Supplemental Table SII) and incubated at 4°C for 30 m. B cells were then washed, resuspended in PBS and analyzed by flow cytometry.

Immunohistochemistry

Human tonsil specimens were fixed in formalin and embedded in paraffin. Tissue sections (6 μm) were mounted onto glass slides. After deparaffinization and re-hydration, slides were processed following a typical staining procedure involving antibodies specific for 14-3-3γ, AID, CD20 or CD3, and then goat anti-mouse or goat anti-rabbit IgG secondary Abs conjugated with horseradish peroxidase-labeled polymers (Dako U.S.A.). After color

development using the DAB+ chromogen (Dako U.S.A.), slides were dehydrated and counterstained with hematoxylin before being examined by microscopy.

Mice

Pi3kr1$^{-/-}$ (*p85α*$^{-/-}$) mice were on the C57BL/6 background, as we described (8), and were maintained in the pathogen-free barrier vivarium at the UC Irvine. Mice used in all experiments were 8–12 weeks of age and without any apparent infection or disease. For immunization, mice were first injected intraperitoneally with 100 μg of NP_{16}-CGG (16 molecules of 4-hydroxy-3-nitrophenyl acetyl coupled to 1 molecule of chicken γ-globulin, Biosearch Technologies) in alum (Imject® Alum, Pierce). All protocols were in accordance to the rules and regulations of the Institutional Animal Care and Use Committee of the University of California, Irvine.

Statistical analysis

Statistical analysis was performed using the Excel® software (Microsoft) to calculate *P* values (paired student *t*-test). *P* values less than 0.05 were considered significant.

Results

14-3-3γ is upregulated in germinal center B cells and is induced by primary stimuli

We first analyzed the expression of the 14-3-3γ isoform in germinal center B cells. 14-3-3γ was highly expressed in human tonsils and upregulated in those $CD20^+$ B cells that expressed AID at high levels (Fig. 1A). Like AID, 14-3-3γ was expressed at higher levels in germinal center B cells ($IgD^-CD38^+CD19^+$ cells in humans and $PNA^{hi}B220^+$ cells in mice) than in non-germinal center B cells by immunoblotting and/or qRT-PCR analyses (Fig. 1B, 1C). To determine the nature of stimuli that induce 14-3-3γ, we stimulated purified naïve IgD^+ B cells, in which 14-3-3γ was expressed at a basal low level, with primary CSR-inducing stimuli or primary plus secondary stimuli. 14-3-3γ together with AID was induced in human and mouse B cells stimulated by CD40 engagement plus IL-4 (Fig. 1D). High 14-3-3γ levels were also induced by TLR ligand LPS, R-848 or CpG ODN, and were not further enhanced by IL-4 or anti–δ mAb/dex, which crosslink the BCR in $Igδ^+$ B cells (Fig. 1D, 1E).

We next analyzed kinetics of 14-3-3γ induction in B cells stimulated by LPS. LPS triggers both TLR and BCR signalings and induce high levels of AID, germline I_H-S-C_H transcription and enrichment of combinatorial histone modifications in the Sγ3 region and, eventually, CSR to IgG3 (8, 30). Induction of *14-3-3γ* by LPS was rapid, peaking (20 – 30 folds) within 3 h of stimulation, and then sustained beyond 48 h (Fig. 2A). At 48 h, the levels of *Aicda* expression and germline Iγ3-Sγ3-Cγ3 transcription peaked and CSR from Sμ to Sγ3 (as quantified by levels of circle Iγ3-Cμ transcripts and post-recombination Iμ-Cγ3 transcripts) was readily detectable. In addition, within 3 h of stimulation by LPS, *14-3-3γ* was induced at levels higher than all nineteen genes we analyzed that were involved in B cell differentiation, such as Irf4, which upregulates AID and CSR (2, 36), and A20, which negatively regulates TLR signalings (37) (Fig. 2B).

Thus, 14-3-3γ is expressed in germinal center B cells and is induced in B cells by primary CSR-inducing stimuli, including CD154 (in the presence of IL-4) and TLR ligands. 14-3-3γ induction is rapid, and is sustained over the period of induction of other molecular events that are critical for CSR, such as AID expression and germline I_H-S-C_H transcription.

The 14-3-3γ promoter has two close TSSs and is highly rich in 5′-CpG-3′ dinucleotide motifs

We next addressed molecular mechanisms underlying the rapid 14-3-3γ induction, starting by identifying critical *cis*–regulatory elements in the *14-3-3γ* locus. By performing comparative gene analysis, we identified in the ~ 50–Kb human and mouse *14-3-3γ* locus two evolutionarily conserved non-coding sequences, which may function as the promoter and 3′ untranslated region (3′ UTR), respectively (Fig. 3A). By using 5′-RACE, we next mapped two dominant TSSs within the putative promoter, with the upstream TSS responsible for 66% of mouse *14-3-3γ* transcripts and downstream TSS for 33% (Fig. 3B and not shown). These two mouse *14-3-3γ* TSSs are only 9-bp apart, and the human *14-3-3γ* promoter is suggested to have one TSS around this region (http://tinyurl.com/8m3jbhp; an anti-sense TSS is also suggested). Thus, the *14-3-3γ* promoter falls within the “sharp” class of promoters (i.e., one or few TSSs), which represents less than 30% of eukaryotic promoters (38). It, however, contains no classical TATA-box or initiator (INR) element that is tightly associated with sharp promoters (38), but rather a high density of 5′-CpG-3′ dinucleotide motifs and a high GC content, the hallmarks of CpG islands (Fig. 3C). CpG islands range from 200-bp to 6-Kb in the genome (39). Notably, the *14-3-3γ* promoter is highly conserved and displays a high density of the 5′-CpG-3′ motif, e.g., 34 and 30 motifs in –120-bp – +80-bp of the TSS(s) – or 34% and 30% of DNA – in the human and the mouse, respectively (Fig. 4). This density of 5′-CpG-3′ is higher than 99.5% of more than 10,000 CpG island-containing promoters (39, 40), which occur in 70% of eukaryotic gene and are mostly “broad” promoters with multiple and spreading-out TSSs (38). In addition, 5′-CpG-3′ dinucleotide motifs are enriched in the *14-3-3γ* 3′ UTR, but not in the coding region or intron, accounting for 15% of 3′ UTR DNA (Fig. 3C).

Thus, the *14-3-3γ* promoter is a unique sharp promoter, as it features a narrow CpG island with one of the highest 5′-CpG-3′ dinucleotide densities, but mediates transcription initiation at only two close TSSs.

14-3-3γ induction is concomitant with enhanced CFP1 and H3K4me3 enrichment in its promoter

Unmethylated 5′-CpG-3′ dinucleotide motifs, as occurring in most CpG island-containing promoters, directly interact with the zinc finger Cys-X-X-Cys (CXXC finger) in proteins such as CXXC finger protein 1 (CFP1, also known as CXXC1) (41). CFP1 is a non-enzymatic (structural) subunit of the COMPASS histone methyltransferase complex, which contains either a mixed-lineage leukemia (MLL) protein (MLL1, MLL2, MLL3 or MLL4) or SET1 (SET1a or SET1b) as the enzymatic subunit and several other non-enzymatic subunits (42). In B cells stimulated by LPS plus anti–δ mAb/dex, CFP1 specifically bound the *14-3-3γ* promoter DNA upstream and downstream of the TSSs (Region 5 and 6, respectively, Fig. 4 and Fig. 5A), but not the 5′-CpG-3′-rich 3′ UTR. CFP1 also bound the *14-3-3γ* promoter in purified resting B cells and in B cells cultured without any primary CSR-inducing stimuli, but at lower levels (Fig. 5A and data not shown). The enhancement of the CFP1 recruitment in B cells undergoing CSR was associated with upregulated CFP1 expression, which increased by 4-fold within 60 min of stimulation by LPS (Fig. 5B).

CFP1 mediates the marking of CpG island-containing promoters by histone 3 lysine 4 trimethylation (H3K4me3), a histone modification that indicates the open chromatin state and marks transcription-competent promoters and first exons (41, 43). The CFP1-occupied *14-3-3γ* promoter was specifically enriched in H3K4me3 at high levels in B cells stimulated by LPS plus anti–δ mAb/dex (Fig. 5C) – lower levels of H3K4me3 enrichment in the promoter region downstream of the TSSs (Region 6) were probably due to destabilization of nucleosomes and loss of histones (44) (data not shown). Consistent with low levels of

14-3-3γ expression in unstimulated B cells, H3K4me3 was detectable at a low level in the *14-3-3γ* promoter, probably resulting from the weak CFP1 binding. Finally, H3K4me1, which preferentially marks enhancers (45), was constitutively enriched in several regions of the *14-3-3γ* locus that were devoid of CFP1 and H3K4me3 (Fig. 5D).

Thus, CFP1 is specifically recruited to the *14-3-3γ* promoter CpG island in B cells upon induction by CSR-inducing stimuli. The upregulation of H3K4me3 enrichment in the *14-3-3γ* promoter are concomitant with rapid 14-3-3γ induction.

NF-κB binds to the 14-3-3γ promoter and regulates 14-3-3γ induction

The highest induction of 14-3-3γ among the 20 selected CpG island-containing genes (Fig. 2B) suggested that *cis*–regulatory elements in addition to CpG islands mediate the rapid 14-3-3γ induction in B cells undergoing CSR. We analyzed putative transcription factor-binding sites using the BioBase TRANSFAC® program (http://www.biobase-international.com/product/transcription-factor-binding-sites) and identified two conserved consensus κB motifs (scored at 0.9 and 1.0, respectively) 23-bp and 88-bp upstream of the TSS(s) and an E protein-binding site (E-box motif; scored at 0.9) downstream of the TSS(s) (Fig. 4). This prompted us to hypothesize that 14-3-3γ induction depends on NF-κB, which is induced in a sustained fashion to mediate AID and CSR induction (8, 23). NF-κB comprises heterodimers activated by the canonical pathway (e.g., the p65/p50 heterodimer) or the non-canonical pathway (e.g., p52/RelB heterodimer). As we have shown, both pathways can be activated by LPS, particularly in the presence of anti−δ mAb/dextran, or CD40 engagement (8). The NF-κB p65 and p52 subunits were recruited to the *14-3-3γ* promoter in B cells stimulated with LPS plus anti−δ mAb/dextran or CD154 plus IL-4, but were virtually absent in the *14-3-3γ* promoter in unstimulated B cells (Fig. 6A and not shown). In addition, p65 was associated with CFP1 on the *14-3-3γ* promoter (Fig. 6B), likely in a macromolecular complex that also contains other components of histone methyltransferases. NF-κB also bound an intronic region (Region 10) and a region in the 3′ UTR (Region 14), both containing putative κB motifs and displaying enrichment of H3K4me1 but not H3K4me3 (Fig. 5 and not shown).

To address the role of NF-κB in 14-3-3γ induction, we inhibited NF-κB activation by using TPCA-1, an inhibitor of IKK-2 in the canonical NF-κB pathway. Recruitment of p65 to the *14-3-3γ* promoter was virtually abolished by TPCA-1 in LPS-stimulated B cells, resulting in more than 80% reduction in 14-3-3γ expression (Fig. 6C, 6D and Supplemental Fig. 1). Induction of 14-3-3γ was also severely impaired in B cells lacking p85α, the major regulatory subunit of PI(3)K (*p85α*$^{-/-}$), due to the critical role of PI(3)K in transducing BCR signaling, including that triggered by anti–Igδ mAb/dex or LPS, to activate both the canonical and the non-canonical NF-κB pathways (8). It was completely abolished in TPCA-1-treated *p85*$^{-/-}$ B cells (Fig. 6D).

Thus, 14-3-3γ induction critically depends on NF-κB, which is activated by the canonical and non-canonical pathways and then recruited to the *14-3-3γ* promoter in B cells undergoing CSR.

E2A transcription factors bind to the 14-3-3γ promoter and synergize with NF-κB to sustain 14-3-3γ induction for CSR

The E-box motif located immediately downstream of the *14-3-3γ* TSSs suggests a role of E2A proteins (E12 and E47) in 14-3-3γ induction in B cells. E2A proteins belong to the class I helix-loop-helix transcription factor members of the E protein family that are essential for B cell and T cell development. E12 and E47 regulate a network of genes that orchestrate B and T cell fates (46), possibly by mediating DNA demethylation in gene

promoters and chromatin remodeling to increase the accessibility to the transcription machinery (47, 48). E2A proteins, which are activated by LPS or BCR crosslinking in mature B cells and play a role in CSR (34), specifically bound the E-box motif in the *14-3-3γ* promoter (Region 6) in B cells stimulated by LPS alone or LPS plus anti–Igδ mAb/dex (Fig. 7A). They also bound this motif in unstimulated B cells, albeit at lower levels.

We next addressed the role of E2A proteins as well as NF-κB in 14-3-3γ induction using luciferase reporter assays in CH12F3 B cells. These transcription factors are induced by CD154, IL-4 and TGF-β to express high levels of AID and undergo CSR to IgA (14). The *14-3-3γ* promoter was highly activated within 3 h of stimulation by CD154, IL-4 and TGF-β and fully activated within 24 h (Fig. 7B). A promoter mutant that lacked the two κB motifs (Mut1) or both the κB and E-box motifs (Mut3) displayed little, if any promoter activity. By contrast, a promoter mutant lacking the E-box motif (Mut2) displayed virtually "normal" activity within 3 h of stimulation, but significantly reduced activity after 24 h, suggesting that E2A proteins are important for sustained 14-3-3γ expression. To confirm this notion, we pre-activated B cells with LPS to induce 14-3-3γ and then used retrovirus transduction to express Id3, which lacked a DNA-binding domain but could heterodimerize with E2A proteins to block them from binding to E-box motifs and mediating transcriptional activation (48, 49). Id3 blocked E2A binding to the *14-3-3γ* promoter, decreased 14-3-3γ transcript and protein levels and inhibited CSR, without altering germline Iγ1-Cγ1 transcription (Fig. 8A–8E) – AID expression was also reduced, consistent with a previous report (34).

These results show that E2A proteins are dispensable for the initial induction of 14-3-3γ mediated by NF-κB. They are, however, important for sustained 14-3-3γ expression.

NF-κB enhances CFP1 and E2A binding to the 14-3-3γ promoter

To gain further insights into the molecular mechanisms underlying the critical role of NF-κB in 14-3-3γ induction, we next addressed the role of NF-κB in regulating the recruitment of CFP1, which can directly interact with NF-κB (50), and E2A, which mediated the sustained *14-3-3γ* expression. In B cells (particularly $p85\alpha^{-/-}$ B cells) treated with TPCA-1, which inhibited NF-κB p65 activation and binding to *14-3-3γ* promoter (Fig. 6D), CFP1 recruitment to and H3K4me3 enrichment in the *14-3-3γ* promoter were impaired (Fig. 9). Likewise, E2A binding to the *14-3-3γ* promoter was decreased.

Thus, NF-κB triggers rapid and sustained 14-3-3γ induction by recruiting/stabilizing CFP1 and E2A to/on the *14-3-3γ* promoter.

Discussion

Here, we have shown that 14-3-3γ was induced by primary CSR-inducing stimuli rapidly and at higher levels, as compared to genes reported to be rapidly induced in a B cell differentiation stage-specific fashion, such as Irf4 and A20. Expression of 14-3-3γ was sustained over the course of CSR induction, consistent with the important role of this adaptor in the targeting of AID. The important role of 14-3-3γ in AID targeting has been shown by our previous ChIP analysis involving $14\text{-}3\text{-}3\gamma^{-/-}$ B cells (29); it is further demonstrated by the CSR rescue in $Aicda^{-/-}$ B cells upon expression of a fusion protein containing 14-3-3γ and AID C-terminal truncation mutant ($AID_{1–190}$) (Mai, T., J. Moehlman, G. Li, Z. Xu and P. Casali. 2012. unpublished), but not upon expression of fusion proteins containing $AID_{1–190}$ and other peptides, such as those from protein kinase inhibitor α, HIV-1 Rev, HTLV-1 Rex, MAP kinase, or Ran binding protein 1 (51). The early induction of 14-3-3γ also highlights the requirement of highly regulated AID targeting for the maintenance of genomic integrity, as over-expression of AID or expression of $AID_{1–190}$ leads to enhanced mutagenesis in non-Ig genes (15, 52, 53). 14-3-3γ induction preceded

germline I_H-S-C_H transcription and the introduction of combinatorial H3K9acS10ph histone modifications in the acceptor S region that will undergo recombination (12). 14-3-3γ docking onto H3K9acS10ph-modified chromatin and its subsequent locking to 5′-AGCT-3′ repeats in the target S regions will stabilize the binding of 14-3-3γ and, therefore, AID to those S regions (28, 30). Finally, upon early induction, 14-3-3γ may play a role in regulating gene expression in B cells undergoing CSR, as suggested by its ability to recognize H3S10ph/S28ph and mediate histone crosstalk (54, 55). 14-3-3γ, however, is dispensable for AID expression, germline I_H-S-C_H transcription and B cells proliferation and viability, as these are largely normal in *14-3-3γ*$^{-/-}$ B cells (29).

Like AID and histone modifying enzymes (8, 30), 14-3-3γ was upregulated in a B cell differential stage fashion and induced by T-dependent and T-independent primary CSR-inducing stimuli, which are the main B cell NF-κB-activating stimuli (12). Accordingly, 14-3-3γ induction is critically dependent on NF-κB, as demonstrated by our findings that the (canonical) p65 and (non-canonical) p52 were recruited to the *14-3-3γ* promoter, the *14-3-3γ* promoter mutants lacking the κB motifs had markedly reduced activities, and 14-3-3γ expression was abrogated in *p85α*$^{-/-}$ B cells treated with the IKK-2 inhibitor TPCA-1. The canonical NF-κB pathway plays a major role in early *14-3-3γ* promoter activation, as suggested by our previous findings that p65 phosphorylation is rapidly induced in B cells (generally within minutes) by CD154 or LPS (8). This NF-κB pathway typically induces rapid but transient gene expression. By contrast, NF-κB activated by the non-canonical pathway mediates sustained gene expression, including 14-3-3γ induction (Fig. 10). Finally, NF-κB may be recruited to an intronic enhancer (Region 10), which was constitutively enriched in H3K4me1 and was devoid of H3K4me3 (45), to further enhance the *14-3-3γ* induction.

Epigenetic modifications are emerging as key regulators of the antibody response, including SHM, CSR, memory B cell differentiation and plasma cell differentiation (28). The time lag of 14-3-3γ induction and those of AID induction and germline I_H-S-C_H transcription in the downstream Igγ, Igε or Igα sub-locus (the Igμ sub-locus is constitutively transcribed) would reflect different epigenetic states of these genes in resting mature B cells. In these cells, the *14-3-3γ* promoter is already bound by CFP1 and enriched for H3K4me3 at low levels, suggesting that it is in a relatively open chromatin state “poised” for the recruitment of NF-κB and the transcription machinery (Fig. 10). By contrast, the *Aicda* gene and I_H (Iγ, Iε and Iα) promoters are in an epigenetic repressed state, as suggested by the DNA hypermethylation as well as low H3 acetylation, H3K4me3, H3K9ac and/or H3S10ph in those regions (30, 56–59). In activated B cells, binding of NF-κB would facilitate the recruitment of the CFP1-containing COMPASS complex for induction of much higher levels of H3K4me3 enrichment (Fig. 10), as indicated by our findings that NF-κB co-localized with CFP1, likely through direct interactions (50), on the *14-3-3γ* promoter in activated B cells. Conversely, CFP1 binding and H3K4me3 enrichment were impaired in B cells treated with TPCA-1. This is reminiscent of the recruitment of chromatin modifying enzymes, such as the H3K9 demethylase Aof1 and H3K27 methyltransferase Ezh2, by transcription factors, including NF-κB, Pax5 and Stat5, to their target genes (60–62). In addition, NF-κB can also upregulate CFP1 expression (30), thereby further augmenting the CFP1 recruitment to the *14-3-3γ* promoter. Finally, knockdown of *Cfp1* in CH12F3 B cells by shRNA significantly inhibits CSR to IgA, as induced by CD154, IL-4 and TGF-β, without affecting AID expression or germline Iα-Cα transcription (27), perhaps resulting from defective AID recruitment/stabilization to/on S region DNA, possibly because of *14-3-3γ* downregulation.

The open chromatin state of the *14-3-3γ* promoter would be promoted by the unusually high density of 5′-CpG-3′ dinucleotide motifs (accounting for more than 30% of DNA), resulting

in not only CFP1 binding but also virtually complete DNA demethylation and nucleosome destabilization (Zan and Casali, unpublished). Such a high density in the relatively short (about 200-bp) promoter region may explain the sharp nature of the *14-3-3γ* promoter, in contrast to most CpG island-containing promoters, which average 1-Kb in size (40). Notably, the *14-3-3γ* promoter, but not the 5′-CpG-3′-rich 3′ UTR, is rich in 5′-CpGG-3′ trinucleotide motifs, which in their unmethylated form are bound by CFP1 with a higher affinity than unmethylated 5′-CpGA/C/T-3′ trinucleotide motifs (63). By contrast, MLL1 and KDM2A, two other proteins that bind to unmethylated 5′-CpG-3′, have not been shown to have a higher affinity for unmethylated 5′-CpGG-3′ (40, 64). Collectively, stabilization by NF-κB and high-affinity binding to 5′-CpGG-3′ trinucleotide motifs may explain the promoter-specific recruitment of CFP1, which would in turn prevent *de novo* 5′-CpG-3′ methylation (40, 65).

In addition to NF-κB, which is ubiquitously expressed and broadly regulates many genes (66), E2A proteins are necessary for sustained 14-3-3γ expression in B cells undergoing CSR, as shown by our luciferase reporter assays of the *14-3-3γ* promoter mutant lacking the E-box motif and Id3 blocking of sustained expression of 14-3-3γ, as already induced by LPS. The location of the E-box motif with the *14-3-3γ* promoter is unique, as it is localized immediately downstream of the TSSs and is flanked by 5′-CpG-3′ motifs, and this unique location might contribute to the TSS sharpness by anchoring the RNA polymerase II pre-initiation complex. E2A transcription factors have been suggested to interact with and recruit the p300/CBP histone acetyltransferase to insert the active histone mark H3K27ac, thereby promoting recruitment of RNA polymerase II and unwrapping of DNA from histones (67–69). These putative E2A activities together with low levels of H3K4me3 in *14-3-3γ* promoter in resting B cells would mediate basal levels of 14-3-3γ expression (Fig. 10). Upon CD40 or TLR engagement, E2A binding to the *14-3-3γ* promoter could be significantly enhanced in an NF-κB-dependent fashion, probably through upregulation of E2A expression, enhanced locus accessibility, and/or interactions with other components in the macromolecular complex assembled on the promoter. Interestingly, it has recently been shown that E2A proteins bind 14-3-3 (70), raising the possibility that E2A proteins can interact with newly induced 14-3-3γ to regulate gene expression.

Overall, our findings on the role of NF-κB and E2A in induction of 14-3-3γ gene expression, together with the previous demonstration of the AID gene activation by a multitude of transcription factors (12), highlight the importance of combinatorial interplay of transcription factors in mediating gene expression in a B cell-specific and B cell differentiation stage-specific fashion. They have lent support to two principles in epigenetic regulation of gene expression: (i) 5′-CpG-3′ motifs and their binding protein CFP1 provide an important link of crosstalk between DNA demethylation and histone modifications; and (ii) recruitment of histone modifying enzymes is mediated by activated transcription factors. Finally, they emphasize the critical role of epigenetic modifications in the specification of biological information output in response to environmental stimuli, e.g., antibody class-switching in response to infection by microbial pathogens.

Supplementary Material

Refer to Web version on PubMed Central for supplementary material.

Acknowledgments

We thank Sohee Lee for excellent technical assistance.

This work was supported by National Institutes of Health grants AI 079705, AI 060573 and AI 105813 (to P.C.), and T.M. was supported by the AI 060573 and T32 CA 009054 training grants.

Abbreviations used in this article

Ab	antibody
AID	activation-induced cytidine deaminase
BCR	B cell receptor
ChIP	chromatin immunoprecipitation
CSR	class switch DNA recombination
DSB	double-strand DNA break
Ig	immunoglobulin
LPS	lipopolysaccharides
MAMP	microbe-associated molecular pattern
H3K4me1	monomethylation of histone 3 lysine 4
H3K4me3	trimethylation of histone 3 lysine 4
NHEJ	non-homologous recombination
SHM	somatic hypermutation
S	switch
TSS	transcription start site
TPCA-1	[5-(p-Fluorophenyl)-2-ureido] thiophene-3-carboxamide

References

1. Goodnow CC, Vinuesa CG, Randall KL, Mackay F, Brink R. Control systems and decision making for antibody production. Nat. Immunol. 2010; 11:681–688. [PubMed: 20644574]
2. Nutt SL, Taubenheim N, Hasbold J, Corcoran LM, Hodgkin PD. The genetic network controlling plasma cell differentiation. Semin. Immunol. 2011; 23:341–349. [PubMed: 21924923]
3. McHeyzer-Williams M, Okitsu S, Wang N, McHeyzer-Williams L. Molecular programming of B cell memory. Nat. Rev. Immunol. 2012; 12:24–34.
4. Bishop GA, Hostager BS. The CD40–CD154 interaction in B cell-T cell liaisons. Cytokine Growth Factor Rev. 2003; 14:297–309. [PubMed: 12787567]
5. Bishop GA. The many faces of CD40: multiple roles in normal immunity and disease. Semin. Immunol. 2009; 21:255–256. [PubMed: 19713124]
6. Xu W, Santini PA, Matthews AJ, Chiu A, Plebani A, He B, Chen K, Cerutti A. Viral double-stranded RNA triggers Ig class switching by activating upper respiratory mucosa B cells through an innate TLR3 pathway involving BAFF. J. Immunol. 2008; 181:276–287. [PubMed: 18566393]
7. Cerutti A, Puga I, Cols M. Innate control of B cell responses. Trends Immunol. 2011; 32:202–211. [PubMed: 21419699]
8. Pone EJ, Zhang J, Mai T, White CA, Li G, Sakakura J, Patel PJ, Al-Qahtani A, Zan H, Xu Z, Casali P. BCR-signaling synergizes with TLR-signaling to induce AID and immunoglobulin class-switching through the non-canonical NF-κB pathway. Nature Commun. 2012; 3:767. (761-712). [PubMed: 22473011]
9. Pone EJ, Xu Z, White CA, Zan H, Casali P. B cell TLRs and induction of immunoglobulin class-switch DNA recombination. Front. Biosci. 2012; 17:2594–2615.
10. Kato L, Stanlie A, Begum NA, Kobayashi M, Aida M, Honjo T. An evolutionary view of the mechanism for immune and genome diversity. J. Immunol. 2012; 188:3559–3566. [PubMed: 22492685]

11. Casali, P. Somatic recombination and hypermutation in the immune system. In: Krebs, JE.; Goldstein, ES.; Kilpatrick, ST., editors. Lewin's Genes XI. Sudbury, MA: Jones & Bartlett; 2013. p. 459-507.
12. Xu Z, Zan H, Pone EJ, Mai T, Casali P. Immunoglobulin class-switch DNA recombination: induction, targeting and beyond. Nat. Rev. Immunol. 2012; 12:517–531. [PubMed: 22728528]
13. Delker RK, Fugmann SD, Papavasiliou FN. A coming-of-age story: activation-induced cytidine deaminase turns 10. Nat. Immunol. 2009; 10:1147–1153. [PubMed: 19841648]
14. Tran TH, Nakata M, Suzuki K, Begum NA, Shinkura R, Fagarasan S, Honjo T, Nagaoka H. B cell-specific and stimulation-responsive enhancers derepress Aicda by overcoming the effects of silencers. Nat. Immunol. 2010; 11:148–154. [PubMed: 19966806]
15. Stavnezer J. Complex regulation and function of activation-induced cytidine deaminase. Trends Immunol. 2011; 32:194–201. [PubMed: 21493144]
16. Maul RW, Saribasak H, Martomo SA, McClure RL, Yang W, Vaisman A, Gramlich HS, Schatz DG, Woodgate R, Wilson DM 3rd, Gearhart PJ. Uracil residues dependent on the deaminase AID in immunoglobulin gene variable and switch regions. Nat. Immunol. 2011; 12:70–76. [PubMed: 21151102]
17. Stavnezer J, Guikema JE, Schrader CE. Mechanism and regulation of class switch recombination. Annu. Rev. Immunol. 2008; 26:261–292. [PubMed: 18370922]
18. Zan H, White CA, Thomas LM, Mai T, Li G, Xu Z, Zhang J, Casali P. Rev1 recruits Ung to switch regions and enhances dU glycosylation for immunoglobulin class switch DNA recombination. Cell Reports. 2012; 2:1220–1232. [PubMed: 23140944]
19. Lieber MR. The mechanism of double-strand DNA break repair by the nonhomologous DNA end-joining pathway. Annu. Rev. Biochem. 2010; 79:181–211. [PubMed: 20192759]
20. Gostissa M, Alt FW, Chiarle R. Mechanisms that promote and suppress chromosomal translocations in lymphocytes. Annu. Rev. Immunol. 2011; 29:319–350. [PubMed: 21219174]
21. Xie P, Poovassery J, Stunz LL, Smith SM, Schultz ML, Carlin LE, Bishop GA. Enhanced Toll-like receptor (TLR) responses of TNFR-associated factor 3 (TRAF3)-deficient B lymphocytes. J. Leukoc. Biol. 2011; 90:1149–1157. [PubMed: 21971520]
22. Litinskiy MB, Nardelli B, Hilbert DM, He B, Schaffer A, Casali P, Cerutti A. DCs induce CD40-independent immunoglobulin class switching through BLyS and APRIL. Nat. Immunol. 2002; 3:822–829. [PubMed: 12154359]
23. Park SR, Zan H, Pal Z, Zhang J, Al-Qahtani A, Pone EJ, Xu Z, Mai T, Casali P. HoxC4 binds to the promoter of the cytidine deaminase AID gene to induce AID expression, class-switch DNA recombination and somatic hypermutation. Nat. Immunol. 2009; 10:540–550. [PubMed: 19363484]
24. Wang L, Wuerffel R, Feldman S, Khamlichi AA, Kenter AL. S region sequence, RNA polymerase II, and histone modifications create chromatin accessibility during class switch recombination. J. Exp. Med. 2009; 206:1817–1830. [PubMed: 19596805]
25. Kuang FL, Luo Z, Scharff MD. H3 trimethyl K9 and H3 acetyl K9 chromatin modifications are associated with class switch recombination. Proc. Natl. Acad. Sci. U.S.A. 2009; 106:5288–5293. [PubMed: 19276123]
26. Daniel JA, Santos MA, Wang Z, Zang C, Schwab KR, Jankovic M, Filsuf D, Chen HT, Gazumyan A, Yamane A, Cho YW, Sun HW, Ge K, Peng W, Nussenzweig MC, Casellas R, Dressler GR, Zhao K, Nussenzweig A. PTIP promotes chromatin changes critical for immunoglobulin class switch recombination. Science. 2010; 329:917–923. [PubMed: 20671152]
27. Stanlie A, Aida M, Muramatsu M, Honjo T, Begum NA. Histone3 lysine4 trimethylation regulated by the facilitates chromatin transcription complex is critical for DNA cleavage in class switch recombination. Proc. Natl. Acad. Sci. U.S.A. 2010; 107:22190–22195. [PubMed: 21139053]
28. Li G, Zan H, Xu Z, Casali P. Epigenetics of the antibody response. Trends Immunol. 2013; 34 In press.
29. Xu Z, Fulop Z, Wu G, Pone EJ, Zhang J, Mai T, Thomas LM, Al-Qahtani A, White CW, Park SR, Steinacker P, Li Z, I. Yates JR, Herron B, Otto M, Zan H, Fu H, Casali P. 14-3-3 adaptor proteins recruit AID to 5'-AGCT-3'-rich switch regions for class switch recombination. Nat. Struct. Mol. Biol. 2010; 17:1124–1135. [PubMed: 20729863]

30. Li G, White CA, Lam T, Pone EJ, Tran DC, Hayama KL, Zan H, Xu Z, Casali P. Combinatorial H3K4acS10ph histone modification in IgH locus S regions targets 14-3-3 adaptors and AID to specify antibody class-switch DNA recombination. Cell Reports. 2013; 5
31. Barreto V, Reina-San-Martin B, Ramiro AR, McBride KM, Nussenzweig MC. C-terminal deletion of AID uncouples class switch recombination from somatic hypermutation and gene conversion. Mol. Cell. 2003; 12:501–508. [PubMed: 14536088]
32. Shinkura R, Ito S, Begum NA, Nagaoka H, Muramatsu M, Kinoshita K, Sakakibara Y, Hijikata H, Honjo T. Separate domains of AID are required for somatic hypermutation and class-switch recombination. Nat. Immunol. 2004; 5:707–712. [PubMed: 15195091]
33. Zan H, Casali P. Regulation of *Aicda* expression and AID activity. Autoimmunity. 2013; 46:83–101. [PubMed: 23181381]
34. Sayegh CE, Quong MW, Agata Y, Murre C. E-proteins directly regulate expression of activation-induced deaminase in mature B cells. Nat. Immunol. 2003; 4:586–593. [PubMed: 12717431]
35. Mai T, Zan H, Zhang J, Hawkins JS, Xu Z, Casali P. Estrogen receptors bind to and activate the HOXC4/HoxC4 promoter to potentiate HoxC4-mediated activation-induced cytosine deaminase induction, immunoglobulin class switch DNA recombination, and somatic hypermutation. J. Biol. Chem. 2010; 285:37797–37810. [PubMed: 20855884]
36. Klein U, Casola S, Cattoretti G, Shen Q, Lia M, Mo T, Ludwig T, Rajewsky K, Dalla-Favera R. Transcription factor IRF4 controls plasma cell differentiation and class-switch recombination. Nat. Immunol. 2006; 7:773–782. [PubMed: 16767092]
37. Kawai T, Akira S. TLR signaling. Semin. Immunol. 2007; 19:24–32. [PubMed: 17275323]
38. Valen E, Sandelin A. Genomic and chromatin signals underlying transcription start-site selection. Trends Genet. 2011; 27:475–485. [PubMed: 21924514]
39. Illingworth RS, Gruenewald-Schneider U, Webb S, Kerr AR, James KD, Turner DJ, Smith C, Harrison DJ, Andrews R, Bird AP. Orphan CpG islands identify numerous conserved promoters in the mammalian genome. PLoS Genet. 2010; 6:e1001134. [PubMed: 20885785]
40. Deaton AM, Bird A. CpG islands and the regulation of transcription. Genes Dev. 2011; 25:1010–1022. [PubMed: 21576262]
41. Thomson JP, Skene PJ, Selfridge J, Clouaire T, Guy J, Webb S, Kerr AR, Deaton A, Andrews R, James KD, Turner DJ, Illingworth R, Bird A. CpG islands influence chromatin structure via the CpG-binding protein Cfp1. Nature. 2010; 464:1082–1086. [PubMed: 20393567]
42. Shilatifard A. The COMPASS family of histone H3K4 methylases: mechanisms of regulation in development and disease pathogenesis. Annu. Rev. Biochem. 2012; 81:65–95. [PubMed: 22663077]
43. Clouaire T, Webb S, Skene P, Illingworth R, Kerr A, Andrews R, Lee JH, Skalnik D, Bird A. Cfp1 integrates both CpG content and gene activity for accurate H3K4me3 deposition in embryonic stem cells. Genes Dev. 2012; 26:1714–1728. [PubMed: 22855832]
44. Ramirez-Carrozzi VR, Braas D, Bhatt DM, Cheng CS, Hong C, Doty KR, Black JC, Hoffmann A, Carey M, Smale ST. A unifying model for the selective regulation of inducible transcription by CpG islands and nucleosome remodeling. Cell. 2009; 138:114–128. [PubMed: 19596239]
45. Heintzman ND, Stuart RK, Hon G, Fu Y, Ching CW, Hawkins RD, Barrera LO, Van Calcar S, Qu C, Ching KA, Wang W, Weng Z, Green RD, Crawford GE, Ren B. Distinct and predictive chromatin signatures of transcriptional promoters and enhancers in the human genome. Nat. Genet. 2007; 39:311–318. [PubMed: 17277777]
46. Lin YC, Jhunjhunwala S, Benner C, Heinz S, Welinder E, Mansson R, Sigvardsson M, Hagman J, Espinoza CA, Dutkowski J, Ideker T, Glass CK, Murre C. A global network of transcription factors, involving E2A, EBF1 and Foxo1, that orchestrates B cell fate. Nat. Immunol. 2010; 11:635–643. [PubMed: 20543837]
47. Maier H, Ostraat R, Gao H, Fields S, Shinton SA, Medina KL, Ikawa T, Murre C, Singh H, Hardy RR, Hagman J. Early B cell factor cooperates with Runx1 and mediates epigenetic changes associated with mb-1 transcription. Nat. Immunol. 2004:1069–1077. [PubMed: 15361869]
48. Kee BL. E and ID proteins branch out. Nat. Rev. Immunol. 2009; 9:175–184. [PubMed: 19240756]
49. Mercer EM, Lin YC, Murre C. Factors and networks that underpin early hematopoiesis. Semin. Immunol. 2011; 23:317–325. [PubMed: 21930392]

50. Ravasi T, Suzuki H, Cannistraci CV, Katayama S, Bajic VB, Tan K, Akalin A, Schmeier S, Kanamori-Katayama M, Bertin N, Carninci P, Daub CO, Forrest AR, Gough J, Grimmond S, Han JH, Hashimoto T, Hide W, Hofmann O, Kamburov A, Kaur M, Kawaji H, Kubosaki A, Lassmann T, van Nimwegen E, MacPherson CR, Ogawa C, Radovanovic A, Schwartz A, Teasdale RD, Tegnér J, Lenhard B, Teichmann SA, Arakawa T, Ninomiya N, Murakami K, Tagami M, Fukuda S, Imamura K, Kai C, Ishihara R, Kitazume Y, Kawai J, Hume DA, Ideker T, Hayashizaki Y. An atlas of combinatorial transcriptional regulation in mouse and man. Cell. 2010; 140:744–752. [PubMed: 20211142]
51. Geisberger R, Rada C, Neuberger MS. The stability of AID and its function in class-switching are critically sensitive to the identity of its nuclear-export sequence. Proc. Natl. Acad. Sci. U.S.A. 2009; 106:6736–6741. [PubMed: 19351893]
52. Robbiani DF, Bothmer A, Callen E, Reina-San-Martin B, Dorsett Y, Difilippantonio S, Bolland DJ, Chen HT, Corcoran AE, Nussenzweig A, Nussenzweig MC. AID is required for the chromosomal breaks in c-myc that lead to c-myc/IgH translocations. Cell. 2008; 135:1028–1038. [PubMed: 19070574]
53. Storck S, Aoufouchi S, Weill JC, Reynaud CA. AID and partners: for better and (not) for worse. Curr. Opin. Immunol. 2011; 23:337–344. [PubMed: 21439803]
54. Winter S, Simboeck E, Fischle W, Zupkovitz G, Dohnal I, Mechtler K, Ammerer G, Seiser C. 14-3-3 proteins recognize a histone code at histone H3 and are required for transcriptional activation. EMBO J. 2008; 27:88–99. [PubMed: 18059471]
55. Zippo A, Serafini R, Rocchigiani M, Pennacchini S, Krepelova A, Oliviero S. Histone crosstalk between H3S10ph and H4K16ac generates a histone code that mediates transcription elongation. Cell. 2009; 138:1122–1136. [PubMed: 19766566]
56. Crouch EE, Li Z, Takizawa M, Fichtner-Feigl S, Gourzi P, Montano C, Feigenbaum L, Wilson P, Janz S, Papavasiliou FN, Casellas R. Regulation of AID expression in the immune response. J. Exp. Med. 2007; 204:1145–1156. [PubMed: 17452520]
57. Fujimura S, Matsui T, Kuwahara K, Maeda K, Sakaguchi N. Germinal center B-cellassociated DNA hypomethylation at transcriptional regions of the AID gene. Mol. Immunol. 2008; 45:1712–1719. [PubMed: 17996946]
58. Yamane A, Resch W, Kuo N, Kuchen S, Li Z, Sun HW, Robbiani DF, McBride K, Nussenzweig MC, Casellas R. Deep-sequencing identification of the genomic targets of the cytidine deaminase AID and its cofactor RPA in B lymphocytes. Nat. Immunol. 2011; 12:62–69. [PubMed: 21113164]
59. Kenter AL. AID targeting is dependent on RNA polymerase II pausing. Semin. Immunol. 2012; 24:281–286. [PubMed: 22784681]
60. van Essen D, Zhu Y, Saccani S. A feed-forward circuit controlling inducible NF-κB target gene activation by promoter histone demethylation. Mol. Cell. 2010; 39:750–760. [PubMed: 20832726]
61. McManus S, Ebert A, Salvagiotto G, Medvedovic J, Sun Q, Tamir I, Jaritz M, Tagoh H, Busslinger M. The transcription factor Pax5 regulates its target genes by recruiting chromatin-modifying proteins in committed B cells. EMBO J. 2011; 30:2388–2404. [PubMed: 21552207]
62. Mandal M, Powers SE, Maienschein-Cline M, Bartom ET, Hamel KM, Kee BL, Dinner AR, Clark MR. Epigenetic repression of the Igκ locus by STAT5-mediated recruitment of the histone methyltransferase Ezh2. Nat. Immunol. 2011; 12:1212–1220. [PubMed: 22037603]
63. Xu C, Bian C, Lam R, Dong A, Min J. The structural basis for selective binding of nonmethylated CpG islands by the CFP1 CXXC domain. Nat. Commun. 2011:227. [PubMed: 21407193]
64. Blackledge NP, Zhou JC, Tolstorukov MY, Farcas AM, Park PJ, Klose RJ. CpG islands recruit a histone H3 lysine 36 demethylase. Mol. Cell. 2010; 38:179–190. [PubMed: 20417597]
65. Cierpicki T, Risner LE, Grembecka J, Lukasik SM, Popovic R, Omonkowska M, Shultis DD, Zeleznik-Le NJ, Bushweller JH. Structure of the MLL CXXC domain-DNA complex and its functional role in MLL-AF9 leukemia. Nat. Struct. Mol. Biol. 2010; 17:62–68. [PubMed: 20010842]
66. Baltimore D. NF-κB is 25. Nat. Immunol. 2011; 12:683–685. [PubMed: 21772275]
67. Creyghton MP, Cheng AW, Welstead GG, Kooistra T, Carey BW, Steine EJ, Hanna J, Lodato MA, Frampton GM, Sharp PA, Boyer LA, Young RA, Jaenisch R. Histone H3K27ac separates

active from poised enhancers and predicts developmental state. Proc. Natl. Acad. Sci. U.S.A. 2010; 107:21931–21936. [PubMed: 21106759]

68. Jin Q, Yu LR, Wang L, Zhang Z, Kasper LH, Lee JE, Wang C, Brindle PK, Dent SY, Ge K. Distinct roles of GCN5/PCAF-mediated H3K9ac and CBP/p300-mediated H3K18/27ac in nuclear receptor transactivation. EMBO J. 2011; 30:249–262. [PubMed: 21131905]
69. Sakamoto S, Wakae K, Anzai Y, Murai K, Tamaki N, Miyazaki M, Miyazaki K, Romanow WJ, Ikawa T, Kitamura D, Yanagihara I, Minato N, Murre C, Agata Y. E2A and CBP/p300 act in synergy to promote chromatin accessibility of the immunoglobulin κ locus. J. Immunol. 2012; 188:5547–5560. [PubMed: 22544934]
70. Teachenor R, Beck K, Wright LY, Shen Z, Briggs SP, Murre C. Biochemical and phosphoproteomic analysis of the helix-loop-helix protein E47. Mol. Cell. Biol. 2012; 32:1671–1682. [PubMed: 22354994]

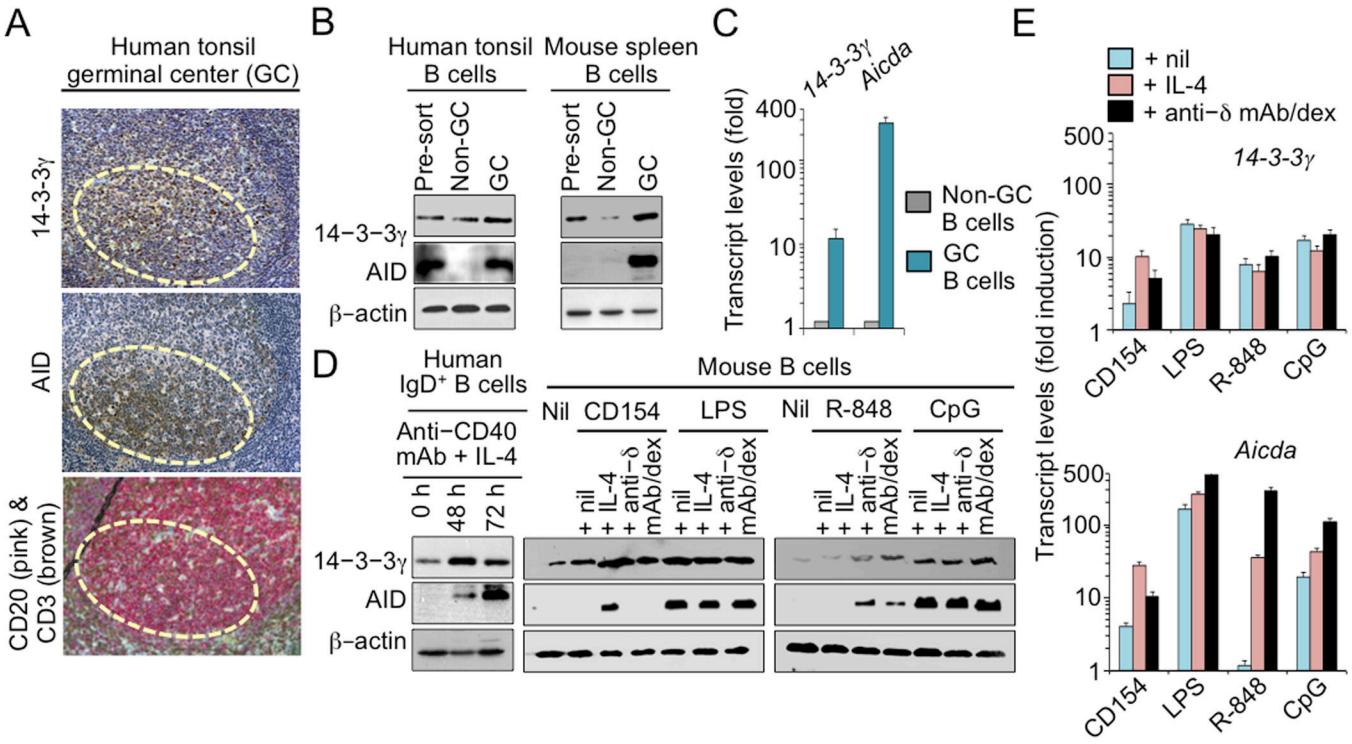

FIGURE 1. 14-3-3γ is upregulated in germinal center B cells *in vivo* and by primary CSR-inducing stimuli *in vitro*

(**A**) Immunohistochemistry analysis of expression of 14-3-3γ (top), AID (middle) and CD20 (a B cell marker, pink signal) together with CD3 (a T cell marker, brown signal, bottom) in serial human tonsil sections. Yellow line-bounded ellipses indicate the germinal center (GC) outer zone, in which B cells express high levels of AID but not Bcl6 (29). Original magnifications: 100X Representative of three independent experiments. (**B**) Immunoblotting analysis of 14-3-3γ and AID expression in human tonsil cells and sorted naive ($IgD^+CD38^-CD19^+$) and GC ($IgD^-CD38^+CD19^+$) tonsil B cells (left panels), as well as in mouse spleen cells and sorted non-GC ($PNA^{lo}B220^+$) and GC ($PNA^{hi}B220^+$) B cells from C57BL/6 mice 14 days after immunization with NP_{16}-CGG (right panels). (**C**) qRT-PCR analysis of expression of *14-3-3γ* and *Aicda* in mouse spleen GC and non-GC B cells, as in (**B**). Data are expressed as ratios of values in GC B cells to those in non-GC B cells (set as 1.2 for graphic purposes). Depicted are mean and s.e.m. of data from three independent experiments. (**D**) Immunoblotting analysis of 14-3-3γ and AID expression in freshly isolated human IgD^+ B cells or B cells stimulated with an agonistic anti–CD40 mAb plus IL–4 for 48 h or 72 h (left panels) or in mouse B cells stimulated with CD154, LPS or TLR ligand R-848 or CpG ODN, alone or in the presence of IL-4 or anti–δ mAb/dex, for 48 h (right panels). (**E**) qRT-PCR analysis of expression of 14-3-3γ and AID in mouse B cells stimulated with CD154, LPS or TLR ligand R-848 or CpG ODN, alone or in the presence of IL-4 or anti–δ mAb/dex, for 24 h. Data are expressed as ratios of values in stimulated B cells to those in unstimulated B cells (mean and s.e.m. of data from three independent experiments).

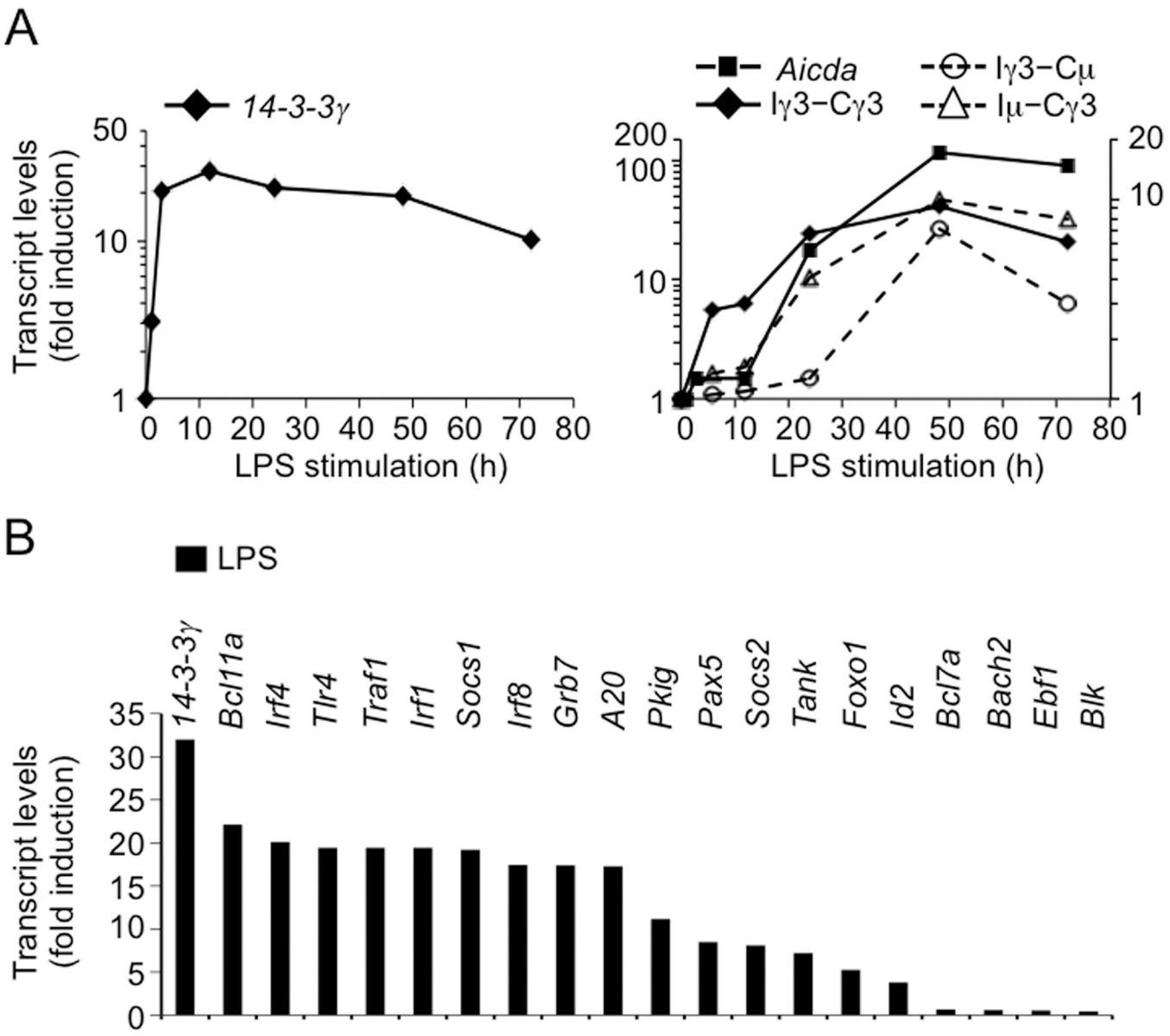

FIGURE 2. 14-3-3γ is induced in B cells rapidly and at higher levels than many B cell differentiation stage-specific genes

(**A**) Kinetics of induction of *14-3-3γ* (left graph), *Aicda* and germline Iγ3-Cγ3 transcripts (right graph, left axis) as well as circle Iγ3-Cμ and post-recombination Iμ-Cγ3 transcript (right graph, right axis) in B cells stimulated with LPS. Data are ratios of expression levels in stimulated B cells at different time-points to those in freshly isolated naïve B cells (0 h, set as 1; at 0 h, the level of *14-3-3γ* transcripts, but not *Aicda* transcripts or germline I_H-S-C_H transcripts, was readily detectable, data not shown). (**B**) qRT-PCR analysis of induction of genes with putative 5′-CpG-3′-rich promoters in B cells stimulated by LPS for 3 h. Data are ratios of expression levels in B cells stimulated by LPS for 3 h to those in freshly isolated B cells (set as 1). Representative of three independent experiments.

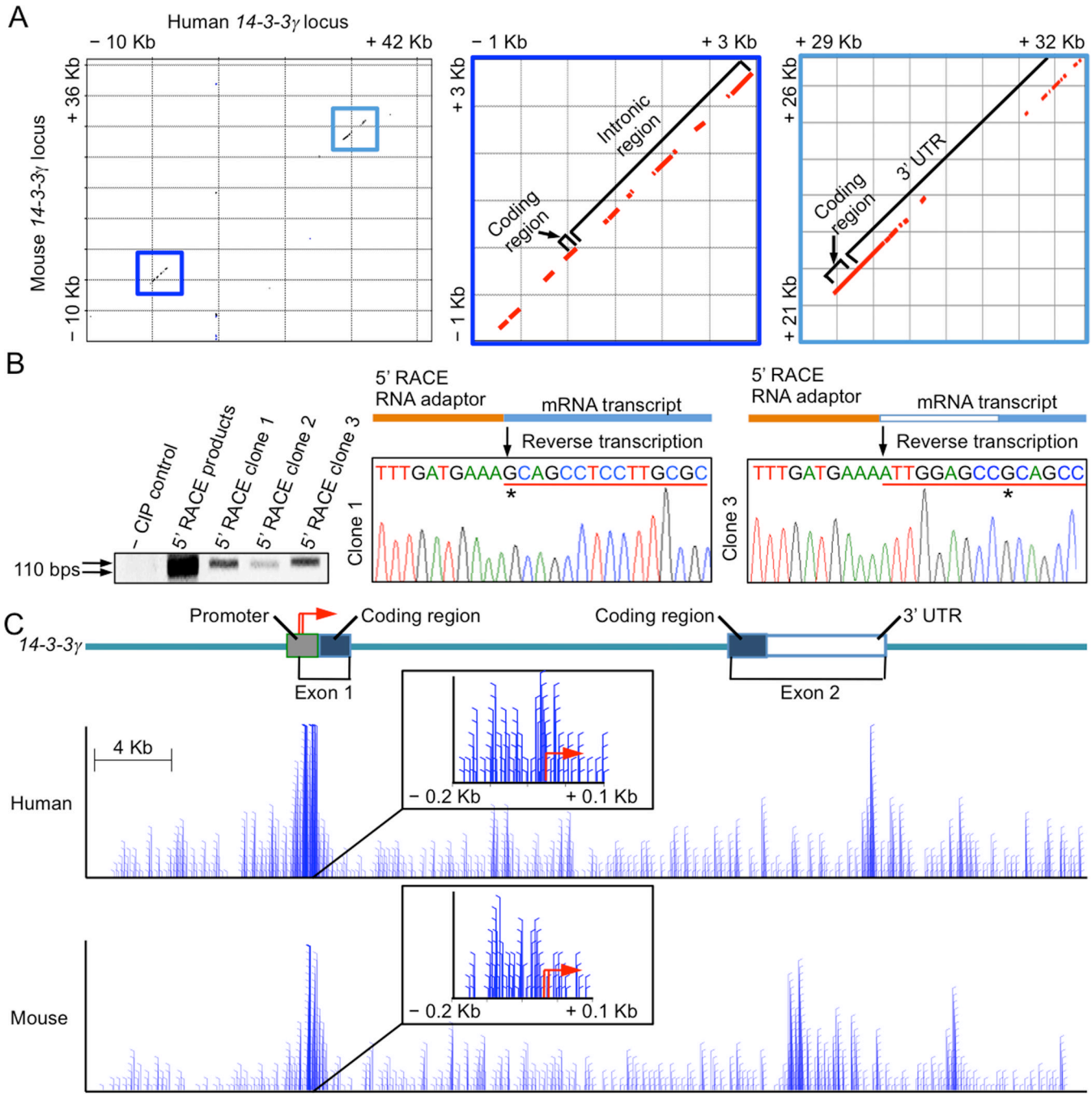

FIGURE 3. The *14-3-3γ* promoter is mapped to a 5′-CpG-3′-rich region

(**A**) Two regions (boxed) with conserved sequences (red lines) in the human and mouse *14-3-3γ* locus (as shown by alignment using the MacVector® software). (**B**) Agarose gel analysis of 5′-RACE products corresponding to the two *14-3-3γ* TSSs (clone 1 and 2, the downstream TSS; clone 3, the upstream TSS) and sequencing analysis of clone 1 and 3 (*: the downstream TSS). (**C**) High densities of 5′-CpG-3′ motifs around the human and mouse *14-3-3γ* promoter (−120-bp – +80-bp of the TSS) and 3′ UTR (3.2-Kb in humans and 2.7-Kb in mice). Each vertical line represents a 5′-CpG-3′ motif (lines are stacked when multiple 5′-CpG-3′ motifs are closely spaced; images were generated by MacVector®). Red arrows,

TSSs; grey bar, the promoter; dark blue bars, the coding region (the two exons are also indicated).

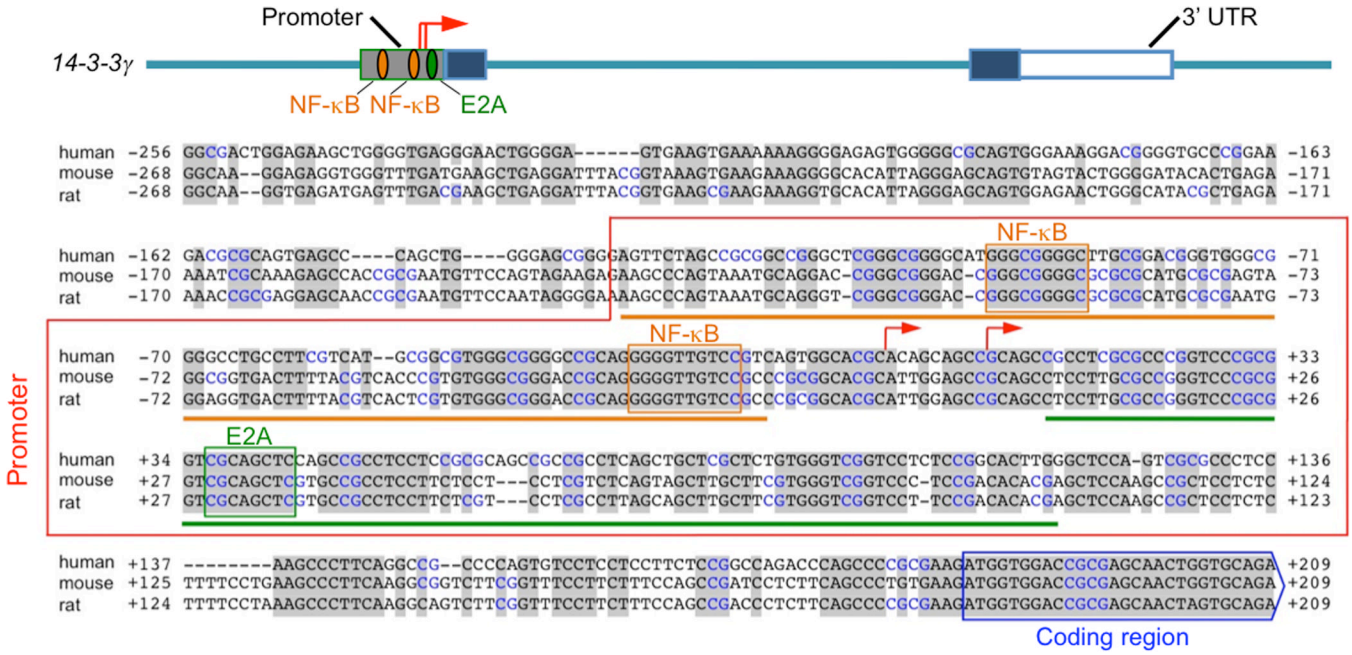

FIGURE 4. The conserved 5′-CpG-3′ -rich *14-3-3γ* promoter contains two κB motifs and one E-box motif

The human, mouse and rat *14-3-3γ* promoters (within the red frame) were aligned by MacVector® (grey marks conserved DNA sequences). 5′-CpG-3′ dinucleotide motifs (in blue) and the promoter DNA upstream (Region 5, orange bar) and downstream (Region 6, green bar) of the two mouse TSSs (red arrows) to be analyzed in ChIP-qPCR are depicted. Also depicted are two putative κB motifs upstream of the TSSs and an E-box motif downstream of the TSSs, as identified by the BioBase TRANSFAC® program (http://www.biobase-international.com/product/transcription-factor-binding-sites).

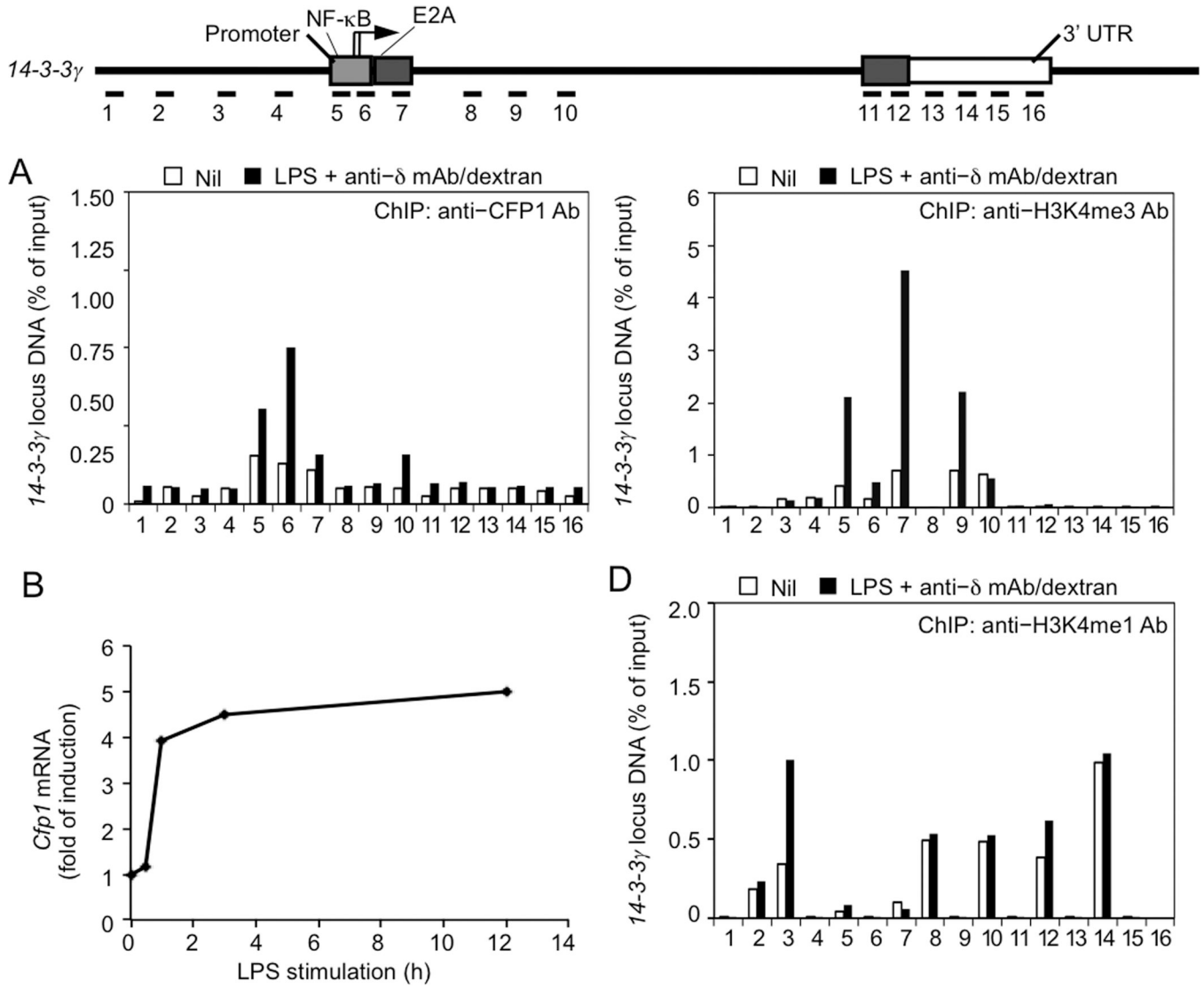

FIGURE 5. Upregulation of CFP1 recruitment to the 5′-CpG-3′ -rich *14-3-3*γ promoter is associated with H3K4me3 induction

(**A**) ChIP-qPCR analysis of CFP1-binding to the selected sixteen conserved regions in the *14-3-3*γ locus (as diagramed in the graph above) in B cells stimulated with nil or LPS plus anti–Igδ mAb/dex for 24 h. (**B**) Kinetics of CFP1 induction in B cells by LPS. Data are expressed as the ratio of expression levels in LPS-stimulated B cells at different time points to those in freshly isolated B cells (0 h, set as 1). (**C, D**) ChIP-qPCR analysis of enrichment of H3K4me3 (**C**, Region 9 might contain a cryptic gene promoter) and H3K4me1 (**D**) in the *14-3-3*γ locus in freshly isolated B cells or B cells stimulated with LPS plus anti−δ mAb/dextran for 24 h, as in (**A**). Representative of three independent experiments.

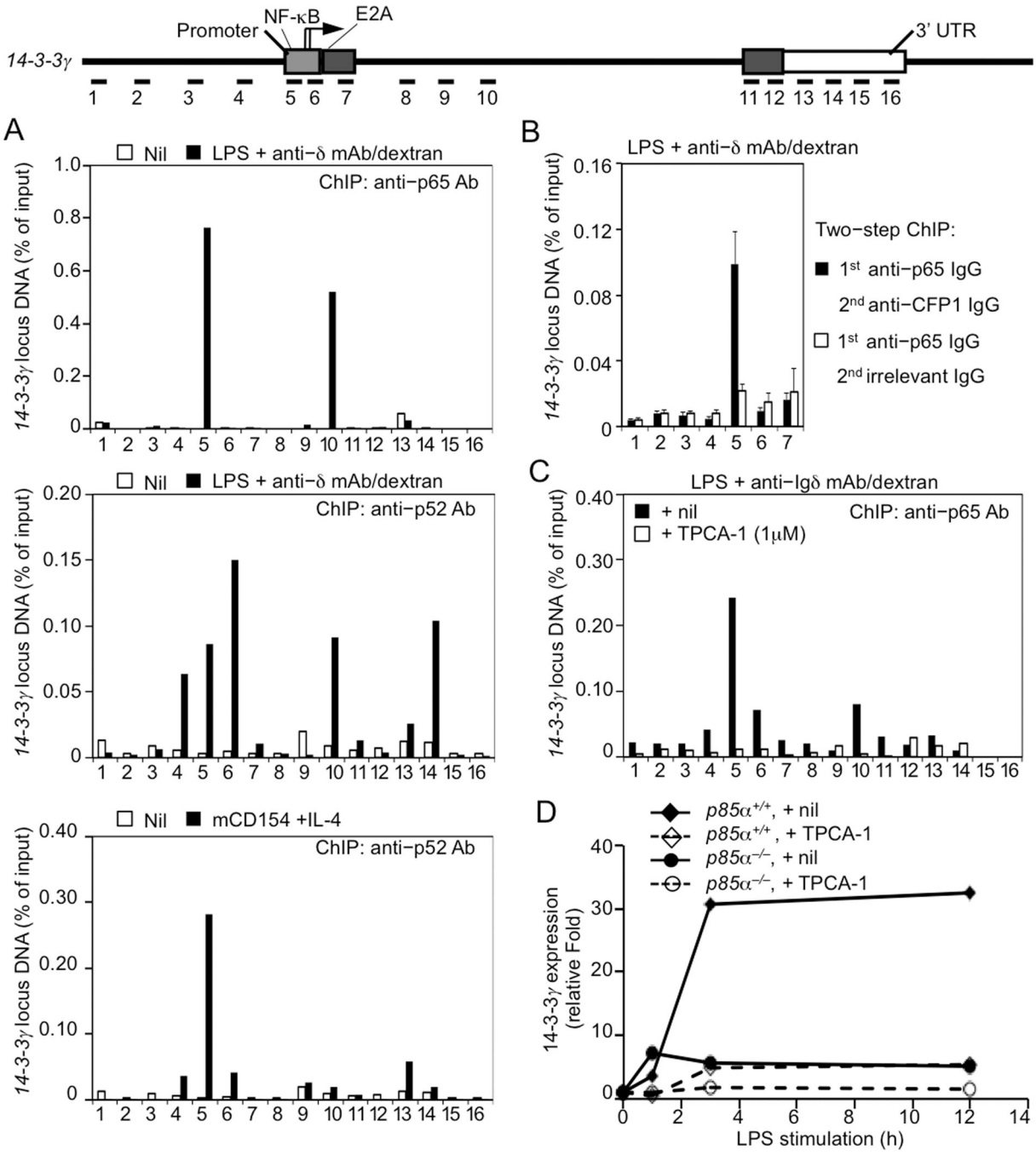

FIGURE 6. NF-κB binds to the *14-3-3γ* promoter and regulates 14-3-3γ induction

(**A**) ChIP-qPCR analysis of NF-κB (p65 of the canonical and p52 of the non-canonical NF-κB pathway, as indicated) binding to the *14-3-3γ* locus (as diagramed in the graph above) in freshly isolated B cells or B cells stimulated with LPS plus anti−δ mAb/dextran or CD154 plus IL-4 for 24 h. (**B**) Sequential ChIP-qPCR analysis of NF-κB (p65; first ChIP) and CFP1 (second ChIP; an IgG Ab with irrelevant specificity was used as the control) binding to the *14-3-3γ* promoter in B cells stimulated with LPS plus anti−δ mAb/dextran for 24 h. (**C**) ChIP-qPCR analysis of NF-κB p65 binding to the *14-3-3γ* locus in B cells treated with nil (DMSO) or TPCA-1 and then stimulated with LPS plus anti−δ mAb/dextran for 24 h. (**D**)

Kinetics of *14-3-3γ* induction in $p85\alpha^{+/+}$ and $p85\alpha^{-/-}$ B cells treated with nil (DMSO) or TPCA-1 and stimulated with LPS. Data are ratios of expression levels in stimulated B cells harvested at different time points to those in freshly isolated B cells (0 h, set as 1). Representative of three independent experiments.

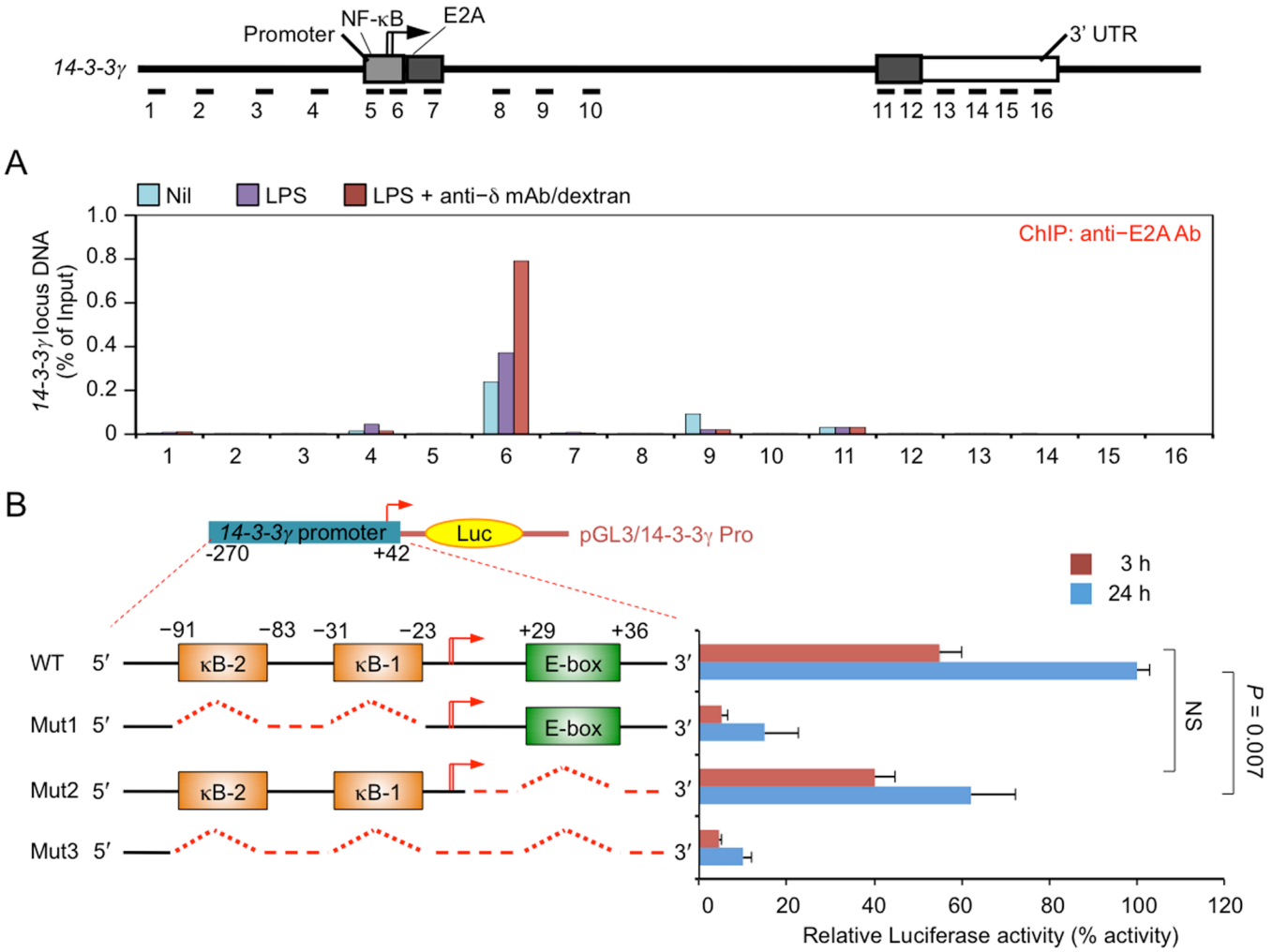

FIGURE 7. NF-κB and E2A mediate different phases of the 14-3-3γ induction

(**A**) ChIP-qPCR analysis of E2A-binding to the *14-3-3γ* locus in B cells stimulated with nil, LPS or LPS plus anti−δ mAb/dextran for 24 h (as diagramed in the graph above). (**B**) Luciferase reporter assays of the activity of the *14-3-3γ* promoter or the *14-3-3γ* promoter mutants (mut1-mut3) that lack the κB and/or E-box motifs, as indicated. Data are expressed as the percentage of expression levels to B cells transfected with wildtype *14-3-3γ* promoter for 24 h (set as 100; mean and s.e.m. of data from three independent experiments; *P* values: t-test; NS, not statistically significant).

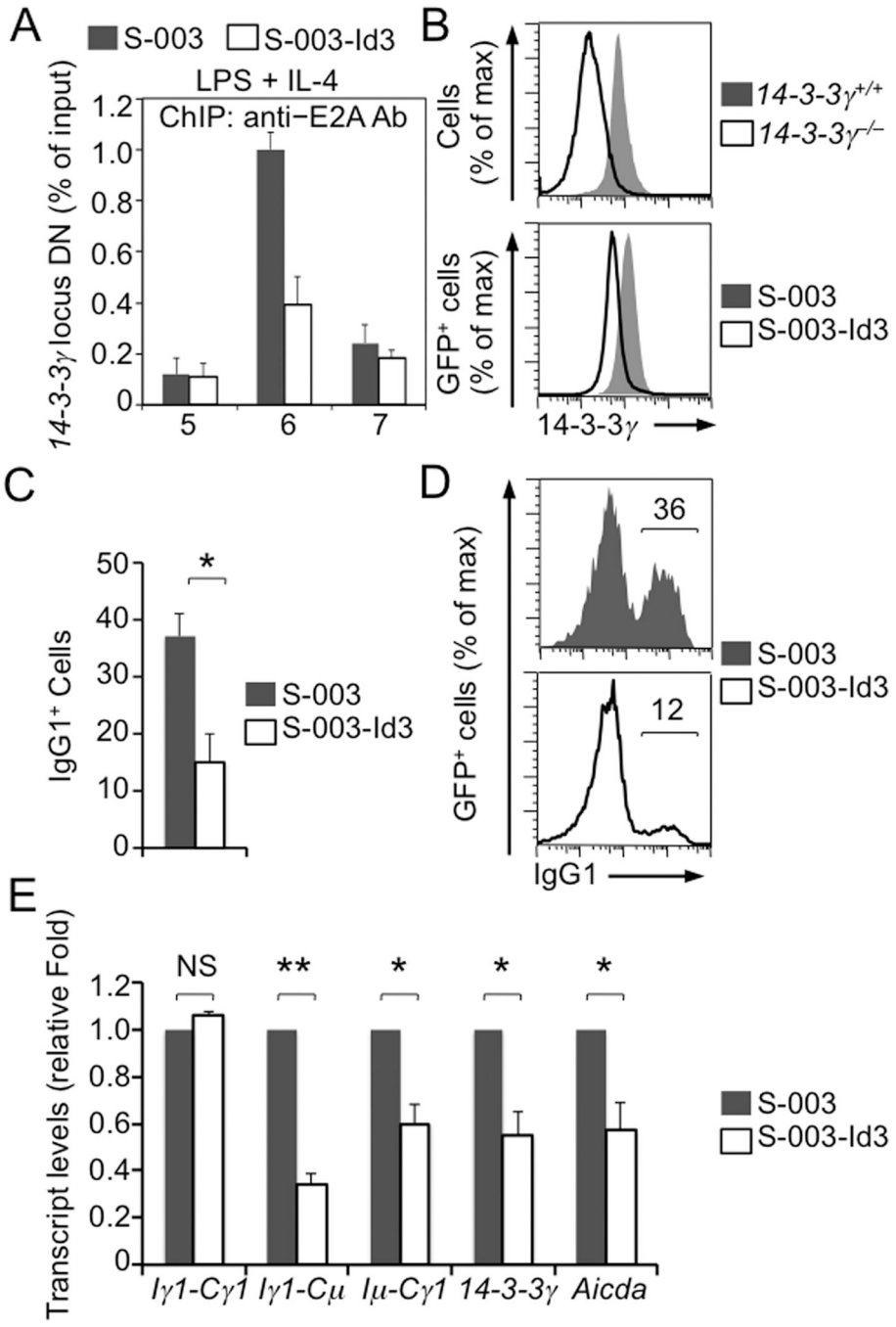

FIGURE 8. E2A sustains 14-3-3γ expression for CSR

(**A**) ChIP-qPCR analysis of E2A binding to the *14-3-3γ* promoter in B cells transduced with S-003 or S-003-Id3 retrovirus and then stimulated with LPS plus IL-4 (bottom) for 48 h. (**B**) Intracellular staining analysis of 14-3-3γ protein levels in *14-3-3γ*$^{+/+}$ and *14-3-3γ*$^{-/-}$ B cells stimulated by LPS (top), and in B cells transduced with S-003 or S-003-Id3 retrovirus and then stimulated with LPS plus IL-4 (bottom) for 48 h. Representative of three independent experiments. (**C, D**) Flow cytometry analysis of the proportion of GFP^{+} B cells that were IgG1^{+} in B cells transduced with S-003 or S-003-Id3 retrovirus and then stimulated with LPS plus IL-4 for 96 h. Histograms in (**C**) depicting the mean and s.e.m. of data from three

independent experiments. (**E**) qRT-PCR analysis of levels of germline Iγ1-Cγ1, circle Iγ1-Cμ, post-recombination Iμ-Cγ1, *14-3-3γ* and *Aicda* transcripts in B cells transduced with S-003 or S00-Id3 and stimulated by LPS plus IL-4 for 48 h. Data are ratios of expression levels in B cells transduced with S003-Id3 to those in B cells transduced with S-003 (set as 1; *P* values: t-test; *, $P < 0.05$; **, $P < 0.01$; NS, not statistically significant).

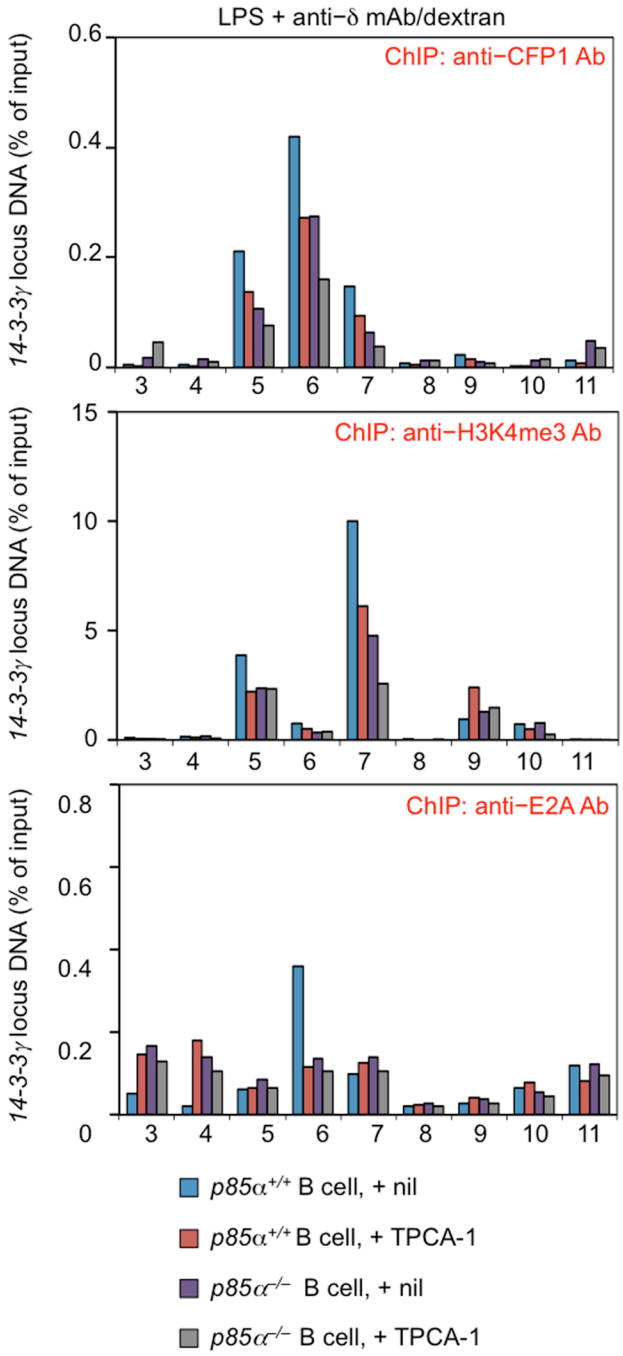

FIGURE 9. NF-κB enhances CFP1 recruitment for H3K4me3 modifications and E2A binding to the *14-3-3*γ promoter

ChIP-qPCR analysis of CFP1-binding, H3K4me3 enrichment and E2A-binding to DNA in the *14-3-3γ* locus (regions three to eleven as diagramed in Figures 5, 6, and 7) in $p85\alpha^{+/+}$ and $p85\alpha^{-/-}$ B cells treated with DMSO (nil) or TPCA-1 and stimulated with LPS plus anti −δ mAb/dextran for 24 h. Representative of three independent experiments.

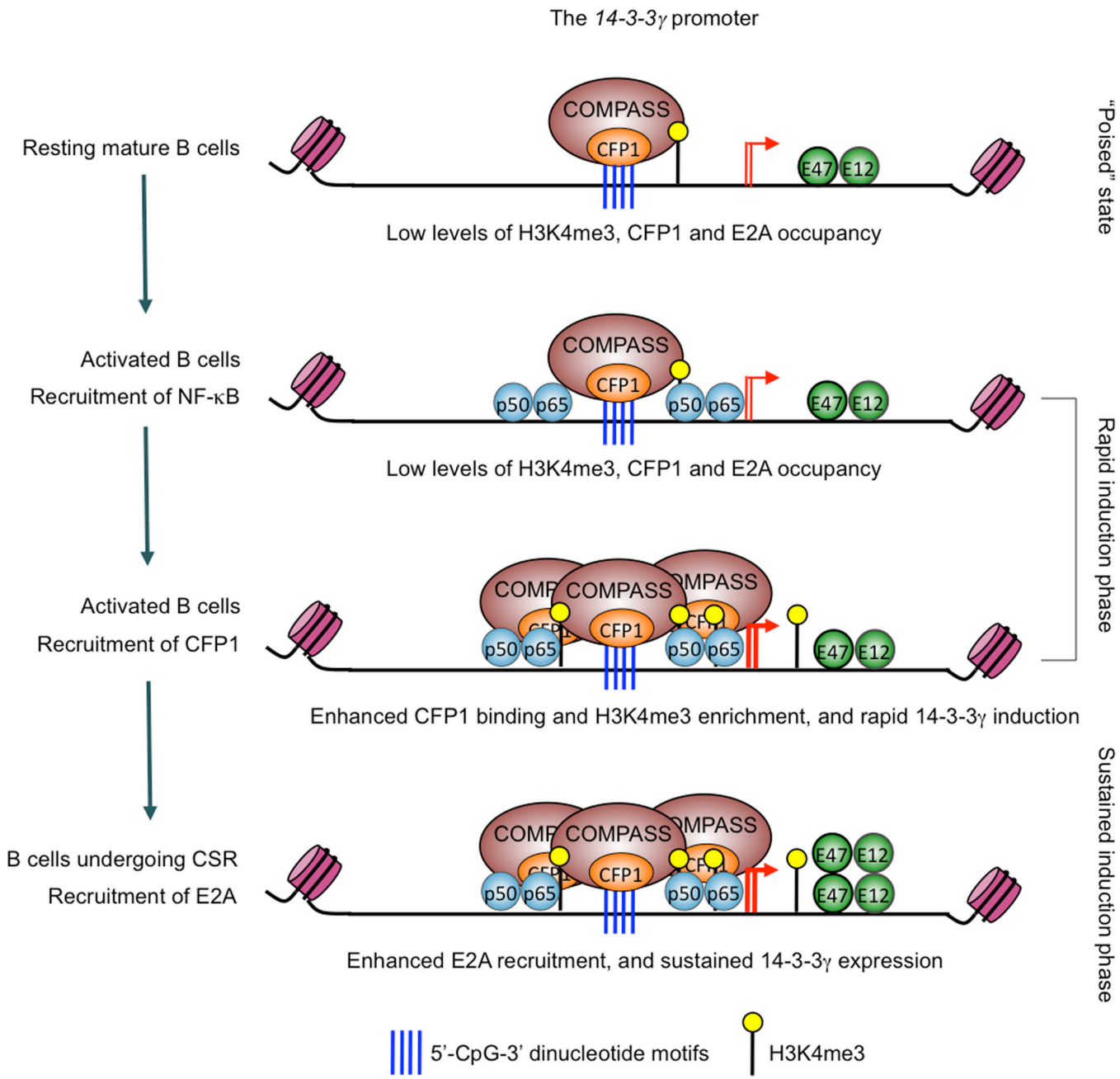

FIGURE 10. Illustration of NF-κB-mediated *14-3-3*γ promoter activation through enhanced CFP1 and E2A binding for rapid and sustained 14-3-3γ induction

In resting mature B cells, the *14-3-3*γ promoter is occupied by CFP1 and marked by H3K4me3 at basal levels, resulting in low levels of 14-3-3γ expression. CFP1 is recruited to the *14-3-3*γ promoter by binding to the high-density 5′-CpG-3′ dinucleotide motifs. CFP1 recruits the COMPASS complex to catalyze the H3K4me3 modification in the promoter, which is also nucleosome-depleted, thereby creating an open chromatin environment to allow access to the transcription initiation machinery. Upon activation by CD40 or TLR engagement, NF-κB (depicted is the p65/p50 heterodimer activated by the canonical pathway) is recruited to the *14-3-3*γ promoter. NF-κB further stabilizes CFP1 to enhance H3K4me3 and mediates the rapid induction of 14-3-3γ through two closely-spaced TSSs.

NF-κB also stabilizes E2A binding to the E-box motif downstream the TSSs for sustained 14-3-3γ expression over the same early period of other molecular events that are critical for CSR, such as AID expression and germline I_H-S-C_H transcription.